

Effects of Tidal Shocks on the Evolution of Globular Clusters

Oleg Y. Gnedin

Princeton University Observatory, Princeton, NJ 08544;
 ognedin@astro.princeton.edu

Hyung Mok Lee

Department of Earth Sciences, Pusan University, Pusan 609-735, Korea;
 hmlee@uju.es.pusan.ac.kr

Jeremiah P. Ostriker

Princeton University Observatory, Princeton, NJ 08544;
 jpo@astro.princeton.edu

ABSTRACT

We present new Fokker-Planck models of the evolution of globular clusters, including gravitational tidal shocks. We extend our calculations beyond the core collapse by adopting three-body binary heating. Effects of the shocks are included by adding the tidal shock terms to the ordinary Fokker-Planck equation: the first order heating term, $\langle \Delta E \rangle$, and the second order energy dispersion term, $\langle \Delta E^2 \rangle$. As an example, we investigate the evolution of models for the globular cluster NGC 6254. Using the *Hipparcos* proper motions, we are now able to construct the orbits of this cluster in the Galaxy. Tidal shocks significantly accelerate both core collapse and the evaporation of the cluster. We examine various types of adiabatic corrections and find that they are critical for accurate calculation of the evolution. Without adiabatic corrections, the destruction time of the cluster is twice as short.

We examine cluster evolution for a wide range of concentration and tidal shock parameters, and determine the region of the parameter space where tidal shocks dominate the evolution. We present fitting formulae for the core collapse time and the destruction time, covering all reasonable initial conditions. The effects of tidal shocks are rapidly self-limiting: as clusters lose mass and become more compact, the importance of the shocks diminishes. This implies that tidal shocks were more important in the past.

Subject headings: stellar dynamics — globular clusters: general — globular clusters: individual (NGC 6254)

1. Introduction

The study of the dynamical evolution of globular clusters has a long and rich history. Spitzer (1987) provides a comprehensive review of the evolution of an isolated cluster. In addition to the internal effects, the external effects produced by the Galactic tidal field are very important. Gnedin & Ostriker (1997) found that tidal shocks contribute at least as much as two-body relaxation to the destruction of the current Galactic sample of globular clusters. In this paper we describe the detailed implementation of tidal shocks in a Fokker-Planck code.

Ambartsumian (1938) and Spitzer (1940) predicted the evaporation of stars from globular clusters to be due to two-body relaxation which causes some stars gain velocity higher than the escape velocity. More careful studies in the 1960s (e.g., Antonov 1962; Lynden-Bell & Wood 1968) revealed that the cluster would experience a catastrophic collapse even in the absence of evaporation, the causes being the negative heat capacity and the conductive transport of heat from the inner to the outer parts of the cluster. As the thermal energy of stars is carried from the inner to the outer parts of the cluster, the run-away process accelerates and leads to a gravothermal catastrophe, or core collapse. Numerical works showed that core collapse is reached in about $14 t_{rh}$, where t_{rh} is the relaxation time at the half-mass radius.

Core collapse will be reversed when a sufficient amount of heating is provided in the core. Most of the proposed heating mechanisms involve binaries, either primordial or formed either by tidal capture or by three-body process. The successive mergers of normal stars and subsequent supernova explosions have also been found to be able to reverse the collapse if the cluster has only normal stars (Lee 1987). After the reversal of core collapse, the evolution of the cluster can be characterized by quasi-static expansion.

The tidal field of the Galaxy affects dynamics of globular clusters in two ways. A steady tidal field imposes a tidal cutoff at the point where the ambient galactic density exceeds the density of stars in the cluster. This tidal boundary accelerates the evaporation of stars (Hénon 1961). Lee & Ostriker (1987) found that the total lifetime of a cluster with short initial relaxation time is $\sim N/200$ orbital periods around the galaxy, where N is the initial number of stars in the cluster. Tidal effects may also cause some rotation as the stars on prograde orbits have higher chances to be ejected than those on retrograde orbits (e.g., Oh & Lin 1992). The time-varying tidal forces cause gravitational shocks when the cluster passes through the disk of the Galaxy (Ostriker, Spitzer, & Chevalier 1972) or comes near the Galactic nucleus (e.g., Spitzer 1987). Finally, Kundic & Ostriker (1994) emphasized that the previously neglected second order tidal shock terms, while not imparting energy to the cluster, can be more important than the first order terms in accelerating cluster evolution.

All of the above processes are included in our Fokker-Planck code. We discuss the implementation of tidal shocks in detail and demonstrate their effects on cluster evolution. We consider both single-mass models and models including a spectrum of stellar masses. Mass segregation (Spitzer 1987) and rapid energy transfer between the stars of different masses lead to an even faster core collapse and destruction of globular clusters.

The only important process that we do not include in our models is mass loss due to stellar evolution. Chernoff & Shapiro (1987) and Chernoff & Weinberg (1990) showed that stellar processes are important at the early stages of cluster evolution, because the mass loss is significant only for the short-lived massive stars. This rapid mass loss can disrupt some weakly concentrated clusters ($c < 0.6$).

We first review the theory of tidal shock in §2. The computations are done using the Fokker-Planck code, which is described in §3. We start with some illustrative cases that show the importance of tidal shock on the evolution of globular clusters in §4. More systematic study for wide ranges of parameter space is covered in §5. Finally, we discuss the implications to the evolution of Galactic star clusters.

2. Review of the Theory of Tidal Shocks

The first and second order theory of the compressive (disk) shocks and tidal (bulge) shocks has been developed by Ostriker, Spitzer, & Chevalier (1972); Spitzer (1987); and Kundic & Ostriker (1994) and

summarized in Gnedin & Ostriker (1997). Below we review the important results for disk shocking. The theory of tidal shocking is discussed in detail in Gnedin, Hernquist, & Ostriker (1998).

In the disk shocking, the phase-averaged first and second order energy changes of stars with initial energy per unit mass E are

$$\langle \Delta E \rangle_E = \frac{2 g_m^2 r^2}{3 V^2} A_1(x), \quad (1)$$

$$\langle \Delta E^2 \rangle_E = \frac{4 g_m^2 v^2 r^2 (1 + \chi_{r,v})}{9 V^2} A_2(x), \quad (2)$$

where g_m is the maximum vertical gravitational acceleration produced by the disk, V is the vertical component of the cluster velocity with respect to the disk, and r and v are the rms position and velocity of stars of energy E . Here $\chi_{r,v}$ is the position-velocity correlation factor, which takes values from -0.25 to -0.57 (see Gnedin & Ostriker 1998).

The first order energy change, $\langle \Delta E \rangle$, causes reduction in the binding energy of the system and leads to the evaporation of the marginally bound stars. The second order change, $\langle \Delta E^2 \rangle$, causes a much larger dispersion of stellar energies, which allows additional stars to leave the cluster. The two effects cooperate and lead to faster dissolution of the cluster.

The adiabatic corrections, $A_1(x)$ and $A_2(x)$, account for conservation of the adiabatic invariants of stars for which the orbital period in the cluster is short compared to the effective duration of the shock,

$$\tau \equiv \frac{H}{V}, \quad (3)$$

where H is the characteristic scale height of the disk. The adiabatic corrections can be approximately described as functions of the only dimensionless parameter,

$$x \equiv \omega(r) \tau. \quad (4)$$

Here ω is the stellar orbital frequency at a given position r ; $\omega(r) \equiv v(r)/r$.

Several approximations have been used to study the adiabatic corrections. (1) The *impulse approximation* is valid for the stars whose motion in the cluster is much slower than the shock, $x \ll 1$. This condition applies to the outer regions of the cluster. There both corrections become unity:

$$A_1(x) = A_2(x) = 1, \quad (x \ll 1). \quad (5)$$

(2) The *harmonic approximation* is valid for the stars which oscillate very quickly in a simple harmonic potential and which are not in resonance with the perturbing force. Following Spitzer (1987),

$$A_1(x) = e^{-2x^2}, \quad A_2(x) = \frac{9}{4 + 5e^{2x^2}}, \quad (x \gg 1; \text{ no resonances}). \quad (6)$$

Here we have modified the second correction from its version in Gnedin & Ostriker (1997) to make it equal unity for $x = 0$. The numeric coefficients are dictated by the asymptotic form for large values of x . (3) The linear theory by Weinberg (1994) includes the possible resonances and predicts a less steep power-law function. In the limit of large τ , the results can be approximated (Gnedin & Ostriker 1998) as:¹

¹This does *not* imply that the results of Weinberg (1994) for short duration shocks are incorrect. The linear theory applies for all values of τ , but the final expressions are complex and cannot be fitted simply.

$$A_1(x) = A_2(x) = (1 + x^2)^{-3/2}. \quad (7)$$

(4) Gnedin & Ostriker (1998) performed N-body simulations of the tidal shock, allowing for the self-consistent oscillations of the cluster potential as it relaxes into a new virial equilibrium. The simple fits to the results are

$$A_1(x) = (1 + x^2)^{-5/2}, \quad A_2(x) = (1 + x^2)^{-3} \quad (8)$$

for the “fast shocks” whose durations are comparable to or smaller than the dynamical time at the half-mass radius: $\tau \lesssim t_{dyn}$. For the “slow shocks”, the results agree with the predictions of the linear theory (eq. [7]).

The first and second order energy changes are of comparable importance. This becomes clear if we define the characteristic shock timescales:

$$t_{sh} \equiv \frac{|E_h|}{dE_h/dt} = P_{\text{disk}} \frac{|E_h|}{\langle \Delta E \rangle_h} \quad (9a)$$

$$t_{sh,2} \equiv \frac{E_h^2}{dE_h^2/dt} = P_{\text{disk}} \frac{E_h^2}{\langle \Delta E^2 \rangle_h}. \quad (9b)$$

Here P_{disk} is the period of cluster’s passage through the Galactic disk. The energy changes $\langle \Delta E \rangle_h$ and $\langle \Delta E^2 \rangle_h$ are evaluated at the half-mass radius R_h , and the characteristic energy E_h is given by the Virial Theorem: $|E_h| = v_{rms}^2/2 \approx 0.2GM/R_h$ (e.g., Spitzer 1987), where M is the mass of the cluster. In the impulse approximation we obtain

$$t_{sh} = \frac{3}{4} P_{\text{disk}} \frac{V^2 \omega_h^2}{g_m^2}, \quad t_{sh,2} = \frac{9}{16} P_{\text{disk}} \frac{V^2 \omega_h^2}{g_m^2}, \quad (10)$$

where $\omega_h \equiv v_{rms}/R_h$ is the rms angular velocity of stars at the half-mass radius. The two time scales are simply related by $t_{sh,2} = \frac{3}{4} t_{sh}$, so that both processes contribute similarly to the destruction of the cluster.

3. The Fokker-Planck Code

We calculate the evolution of globular clusters using an orbit-averaged isotropic Fokker-Planck code descended from Cohn (1979, 1980). The code has been modified by Lee & Ostriker (1987) and Lee, Fahlman, & Richer (1991) to include the tidal boundary and three-body binary heating. Stars beyond the tidal boundary do not escape instantaneously, but follow instead a continuous distribution function $f(E)$, as described in Lee & Ostriker (1987). This accounts for the balance of the internal and external forces at the tidal radius. Therefore, those stars only drift slowly away from the cluster. The tidal field is assumed to be spherically symmetric, which is a weakness of the one-dimensional code (for a discussion see Lee & Goodman 1995). We also assume that the cluster fills its Roche lobe and require that the mean density within the tidal radius remain constant throughout the cluster evolution.

The heating of stars, which reverses core collapse, is provided by three-body binaries. They are included explicitly without following their actual formation and evolution, according to the prescription by Cohn (1985). Ostriker (1985) argued that the tidally captured binaries are probably more dynamically important for massive clusters. Whether tidal capture leads to a hard binary which contributes to stellar ejection after a close encounter or whether it leads (more often) to a merger which causes mass loss following stellar evolution, the outcome is the same. Lee (1987) showed that the merger of stars would give a nearly identical dynamical effect to the cluster because the massive stars formed in the merger would evolve off rapidly.

Both processes cause indirect heating by the ejection of mass. The situation becomes more complicated if we allow for the existence of primordial binaries and massive degenerate stars. The existence of massive remnant stars, such as neutron stars, could cause three-body binaries to be more important than tidal capture binaries (Kim, Lee & Goodman 1998). However, many aspects of the evolution after core collapse are independent of the actual energy source (Hénon 1961; Goodman 1993).

We include the effects of tidal shocks by modifying the diffusion coefficients in the Fokker-Planck equation. We assume that the first and second order energy changes due to the shocks are known as the function of energy, E , and position, r . We now re-derive the Fokker-Planck equation in order to define the diffusion coefficients corresponding to the shocks.

Let $\Psi(E, \Delta E) d\Delta E$ be the probability of scattering of a star of energy E by the amount $[\Delta E, \Delta E + d\Delta E]$. N-body simulations (Gnedin & Ostriker 1998) show that the probability distribution is nearly Gaussian:

$$\Psi(E, \Delta E) d\Delta E = \frac{1}{\sqrt{2\pi\langle\Delta E^2\rangle}} e^{-\frac{1}{2}\frac{(\Delta E - \langle\Delta E\rangle)^2}{\langle\Delta E^2\rangle}} d\Delta E, \quad (11)$$

where both $\langle\Delta E\rangle$ and $\langle\Delta E^2\rangle$ are functions of energy E . Let $N(E)dE$ be the number of stars in the energy range $[E, E + dE]$. The time evolution of $N(E)$, in the absence of two-body relaxation and binary heating, can be described by the following equation

$$N(E, t + \Delta t) = \int N(E - \Delta E, t) \Psi(E - \Delta E, \Delta E) d\Delta E, \quad (12)$$

where the energy changes by the amount ΔE in the time interval Δt . Expanding this equation in a series over ΔE and Δt , we obtain the usual form of the Fokker-Planck equation

$$\frac{\partial N(E)}{\partial t} = -\frac{\partial}{\partial E} \{N(E) \langle\mathcal{D}_t(\Delta E)\rangle_V\} + \frac{1}{2} \frac{\partial^2}{\partial E^2} \{N(E) \langle\mathcal{D}_t(\Delta E^2)\rangle_V\}, \quad (13)$$

where $\langle\mathcal{D}_t(\Delta E)\rangle_V$ and $\langle\mathcal{D}_t(\Delta E^2)\rangle_V$ are the orbit-averaged diffusion coefficients of the first and second order. They are defined by

$$\langle\mathcal{D}_t(\Delta E)\rangle_V \equiv \frac{\int_0^{r_{max}} \langle\mathcal{D}_t(\Delta E)\rangle vr^2 dr}{\int_0^{r_{max}} vr^2 dr}, \quad (14)$$

and

$$\langle\mathcal{D}_t(\Delta E^2)\rangle_V \equiv \frac{\int_0^{r_{max}} \langle\mathcal{D}_t(\Delta E^2)\rangle vr^2 dr}{\int_0^{r_{max}} vr^2 dr}, \quad (15)$$

where $\langle\mathcal{D}_t(\Delta E)\rangle$ and $\langle\mathcal{D}_t(\Delta E^2)\rangle$ are the average rates of change in energy and its dispersion, respectively, per unit volume at a given location r , and r_{max} is the maximum radius allowed for a star of energy E . Given equations (1) and (2) for the energy changes and equation (11) for their distribution function, we define

$$\langle\mathcal{D}_t(\Delta E)\rangle_{sh} \equiv \int \frac{\Delta E}{\Delta t} \Psi(E, \Delta E) d\Delta E = \frac{\langle\Delta E\rangle}{\Delta t}, \quad (16)$$

$$\langle\mathcal{D}_t(\Delta E^2)\rangle_{sh} \equiv \int \frac{(\Delta E)^2}{\Delta t} \Psi(E, \Delta E) d\Delta E = \frac{\langle\Delta E^2\rangle + \langle\Delta E\rangle^2}{\Delta t}. \quad (17)$$

The bulge and disk tidal shocks are applied at the time step when the cluster is at its perigalacticon or crosses the Galactic disk, respectively. The diffusion coefficients are normalized to the current time step,

Δt , so as to produce the right amount of heating per event. The shocks are repeated every orbital period of the cluster.

The time step was chosen such that both mass and central density change by no more than 1% between time steps,

$$\Delta t = 0.01 \times \min[(d \ln \rho/dt)^{-1}, (d \ln M/dt)^{-1}]. \quad (18)$$

Lee & Ostriker (1993) suggested that such a time step should be sufficient for an accurate calculation of the cluster evolution, both before and after core collapse. We compare our results without tidal shocking with those of Quinlan (1996), who used the same time step for the potential re-computation but broke it down into 32 sub-steps for updating the distribution function (the “Fokker-Planck steps”). We found a measurable difference in the core collapse times only for very concentrated clusters, with the initial concentration $c \gtrsim 2.5$. For these clusters an even smaller time step may be required, although our results never differ by more than 30% (cf. Figure 17).

As described below, in order to incorporate correctly the tidal shock effects into the code, the shock diffusion coefficients should be applied separately from the relaxation terms, and the potential should be recomputed accordingly thereafter (an alternative approach has been suggested by Johnston, Hernquist & Weinberg 1998). It seems awkward, though still possible, to include a set of Fokker-Planck steps for every potential time step in this scheme, as Quinlan (1996) did for the isolated clusters. We chose not to do it and therefore we had the potential updated every time the distribution function was changed. Since our time step (eq. [18]) gives very good accuracy for most of the cluster models we compute, we did not change it specifically for high concentration clusters. The resulting error should in any case be small.

3.1. Comparison with N-body simulations

Self-consistent N-body simulations, reported in Gnedin & Ostriker (1998), produce accurate expressions for the ensemble-averaged first and second order energy changes in a tidal shock event. Despite the algorithmic differences between the Fokker-Planck and N-body modeling, we have tried to reproduce the exact effects of tidal shocks in the Fokker-Planck code.

The general procedure for advancing the distribution function (DF) in time consists of two parts (Cohn 1979). The first part introduces the first and second order changes of the DF as a solution of the Fokker-Planck equation. The second part updates the cluster potential by solving Poisson’s equation with the density following from a new DF. During the second step, the DF is kept constant as a function of the stars’ adiabatic invariants and is therefore changed as a function of energy. This procedure is no longer correct when treating tidal shocks, which occur on a short enough timescale to change adiabatic invariants.

Including the diffusion coefficients responsible for tidal shocks, we find that in order to reproduce the N-body results, we need to apply the above procedure for advancing the DF separately for shocks and for ordinary relaxation. In a time step when the cluster passes through the Galactic disk or close to the Galactic center, we first apply the shock diffusion coefficients and update the DF. Since a single tidal shock usually has a timescale comparable to the dynamical time of cluster stars, the adiabatic invariants may change. Therefore, we solve Poisson’s equation for the DF fixed as function of energy. Specifically, since the potential is changed and the energy grid is renormalized, we require that in each energy bin the new energy distribution, N_{new} , scale with the new energy grid, $E_{new} = E + \Delta E$, as

$$N_{new}(E_{new}) dE_{new} = N(E) dE, \quad (19)$$

where $N(E)$ is the energy distribution before the potential recalculation. We have checked that the above procedure reproduces well the N-body results for a range of shock amplitudes. Figure 1 shows the change in the energy distribution, $N(E)$, after a single shock in a test cluster. The agreement between the Fokker-Planck and N-body results is reasonably good. Also, Figure 1 shows that the previous procedure for updating the DF for the fixed adiabatic invariants departs much more strongly from the N-body results than does our new prescription.

Another effect demonstrated by N-body simulations is a slight decrease in the shock-induced energy dispersion subsequent to and caused by the potential fluctuations following the shock. This paradoxical “refrigeration effect” persistently survived all our tests and seems to be real (see Gnedin & Ostriker 1998). However, the magnitude of the dispersion decrease is relatively small, which led us to ignore it in the present calculations. Once the nature of this effect is understood better, it should also be included in globular cluster models.

4. Typical Evolution of a Single Cluster

We consider now a detailed evolution of globular cluster models. For the most part, we study single-mass models and then briefly investigate the effect of a spectrum of stellar masses.

With the new data on proper motions from *Hipparcos*, it is now possible to reconstruct full three-dimensional velocities for some of the Galactic globular clusters (Odenkirchen et al. 1997) and to build realistic models of their evolution. We use the inferred orbital parameters for NGC 6254 and calculate its orbits in an analytic potential of the Galaxy from Allen & Santillan (1991). The orbits are of the rosette type (Figure 2) with a small eccentricity, $e = 0.21$. The cluster moves around the Galaxy with a period of about 1.4×10^8 yr, during which it passes next to the Galactic center every 9.5×10^7 yr and crosses the Galactic disk every 5.3×10^7 yr. The period ratio differs from the expected factor of two due to slow precession of the orbit around the center.

4.1. Single Mass Models

The observed structure of NGC 6254 is well characterized by a King model (King 1966) with the concentration $c = 1.4$, or the structural parameter $W_0 = 6.55$. The mass of the cluster is $2.25 \times 10^5 M_\odot$, assuming a constant mass-to-light ratio $M/L_V = 3$ in solar units. First, we consider in detail a model composed of stars of the same mass, $m_* = 0.7 M_\odot$. The important parameters of the model are summarized in Table 1.

We implement both disk and bulge shocks in our integration. The models differ in the way the shocks are included: no tidal shocks, steady tidal field and relaxation only (*case 0*); the first order tidal shocks with ΔE term only (*case 1*); the second order tidal shocks with ΔE^2 term only (*case 2*); and the full tidal shocks with both ΔE and ΔE^2 terms (*case 3*).

The orbits of NGC 6254, constructed using the *Hipparcos* data, show that the amplitude of tidal shocks varies with time approximately as a Gaussian function. This satisfies the conditions under which the N-body adiabatic corrections were calculated.

An important observable of the cluster evolution is the mass-loss due to tidal shocks and due to the

direct escape of high-velocity stars. Figure 3 shows the run of the cluster mass with time. As is well-known, the mass of a tidally limited cluster goes to zero in an approximately linear fashion. A convenient choice is to express time t in the units of the initial half-mass relaxation time $t_{rh,0}$ (eq. [21]). Two-body relaxation leads to destruction of the cluster in about $32t_{rh,0}$. Note that due to numerical problems, the cluster loses its stability and dissolves into the sea of background stars before its mass reaches exact zero. Usually the code fails to re-calculate the cluster potential when the mass falls to about 1% – 4% of the initial mass. However, we can extrapolate through the last few points in order to estimate the hypothetical time when the cluster mass vanishes. The disruption time obtained this way will be an overestimate of the real disruption time, but all other estimates would suffer from a personal choice. Thus, in the rest of the paper we use the extrapolation of our calculations as the destruction time t_d .

The destruction time is significantly reduced when we include the gravitational shocks. Ignoring shocks, the time to total destruction is $32t_{rh,0}$. The energy shift term alone reduces t_d to $26t_{rh,0}$, and the shock-induced relaxation brings it to about $24t_{rh,0}$. To access the importance of the two shock terms separately, we turn off the energy shift and check how the shock-induced relaxation affects the cluster evolution. The second order effect leads to an enhanced mass loss, relative to the relaxation case, for most of the evolution. This effect is not as strong as the first order effect due to limiting adiabatic corrections, which we investigate in more detail later². For comparison, we show the mass loss that would have been due to the shock-induced relaxation if it had not had adiabatic corrections (impulse approximation). The effect reduces the destruction time of the cluster by about a half.

An important feature of tidal shocks is the mass loss at the early stages of the evolution of the cluster, before core collapse. In the pure relaxation case, the mass-loss is slow before core collapse and linear in time after it. The first theoretical calculations of the probability of stars' escape from the cluster through two-body relaxation (Ambartsumian 1938; Spitzer 1940) gave

$$\xi_e \equiv -\frac{t_{rh}(t)}{M(t)} \frac{dM}{dt} = 0.0074, \quad (20)$$

where t_{rh} is the half-mass relaxation time (Spitzer & Hart 1971):

$$t_{rh} = 0.138 \frac{M^{1/2} R_h^{3/2}}{G^{1/2} m_* \ln(\Lambda)}. \quad (21)$$

Here M is the current cluster mass, R_h is the half-mass radius, m_* is the average stellar mass, and $\ln(\Lambda) = \ln(0.4N)$ is the Coulomb logarithm, N being the number of stars in the cluster. Detailed calculations of the tidally-truncated cluster by Hénon (1961) gave a larger value, $\xi_e \approx 0.045$.

Spitzer & Chevalier (1973) used Monte-Carlo simulations for several models of globular clusters and found $\xi_e = 0.05$ for $R_t/R_h = 3.1$, and $\xi_e = 0.015$ for $R_t/R_h = 9.3$, where R_t is the tidal radius of the cluster. Based upon those simulations, Aguilar, Hut, & Ostriker (1988; hereafter AHO) proposed the following fitting formula for the time to disruption, t_d :

$$t_d = \left(0.15 \frac{R_h}{R_t} \right)^{-1} t_{rh,0}, \quad (22)$$

²The effect of the second order term is reduced relative to the results of Gnedin & Ostriker (1997) by inclusion of the correlation factor $(1 + \chi_{r,v})$ (eq. [2]). At each time step, we calculate the value of $\chi_{r,v}(E; c)$ using the fitting formula from Gnedin & Ostriker (1998).

where $t_{rh,0}$ is the initial relaxation time. For NGC 6254, the disruption time predicted by AHO would be about $52t_{rh,0}$, whereas we see that the cluster dissolves in $32t_{rh,0}$ even without tidal shocks. In general, we find that AHO’s formula overestimates the actual disruption time for clusters by a factor of several.

We compare the previous results for the escape probability ξ_e with our Fokker-Planck calculations in Figure 4. In the relaxation model (*case 0*), ξ_e rises essentially monotonically through core collapse and until destruction of the cluster, reaching and exceeding Hénon’s value only in the late stages of the evolution. On the contrary, in the shock-dominated models the escape probability is very high in the beginning, when tidal shocks efficiently remove stars from the outer parts of the cluster. The mass loss then slows down and conforms to the relaxation rate soon before core collapse. Then again, ξ_e rises with time to reach Hénon’s self-similar value. This later increase caused primarily by the declining mass of the cluster, since the mass loss rate is almost constant in the post core-collapse cluster.

The cluster structure can be described in terms of the characteristic radii, such as the *core radius*, reflecting compactness of the cluster; the *tidal radius*, confining all stars bound to the cluster; and the *half-mass radius*, which is intermediate and related to the total cluster energy. Figure 5 shows the evolution of these parameters, normalized to the initial core radius. Core radii for all models drop to extremely small values at the point of core collapse. The core-collapse time t_{cc} is about $13t_{rh,0}$ for the relaxation case, in agreement with Lee & Ostriker (1987) and Quinlan (1996). Tidal shocks speed up core collapse significantly: $t_{cc} = 10t_{rh,0}$ in *case 1*, and is still smaller when we include the shock-induced relaxation term. The half-mass radius changes only by a factor of two over the whole cluster lifetime, which indicates that core collapse affects only a small fraction of stars. The tidal radius decreases slightly, reflecting the gradual mass loss from the cluster.

Figure 6 illustrates core collapse more clearly. The central density of the cluster, ρ_c , rises by nine orders of magnitude before the collapse is halted by a production of three-body binaries at the very dense center of the cluster. The energy released from the binaries eventually reverses the collapse. The cluster consequently expands, though the central density still remains very high (about four orders of magnitude higher than initially). The actual value of ρ_c at the core bounce and post-collapse phase depends on the specific heating mechanism. A stronger heating rate gives a lower central density during the post-collapse phase.

The cluster concentration, $c \equiv \log_{10}(R_t/R_c)$, is closely related to the central density. Since the tidal radius R_t decreases slowly with time as $M^{1/3}$, the concentration varies roughly as $\log \rho_c$.

Core collapse provides a very useful yardstick for cluster evolution. Even in the presence of tidal shocks, the evolution of the models is similar when the units of time are scaled to the core collapse time. Figure 7 illustrates this point. The central density for the models 0–3 varies almost identically with t/t_{cc} . Therefore, we can use this scaling to parameterize cluster evolution. The destruction time is an almost constant multiple of the core collapse time, $t_d \approx 2.5t_{cc}$.

The post collapse evolution of globular clusters depends on the concentration and the remaining mass. The self-similar solution by Hénon (1961) for tidally-limited clusters can be expressed (Goodman 1993) as follows:

$$t_d - t = 22.4 t_{rh}(t), \quad (23)$$

where $t_d - t$ is the time to disruption at time t . Figure 8 shows that the self-similar limit is approached at late stages of the cluster evolution, but for the most part, equation (23) underestimates time to destruction by about 50%.

4.1.1. Comparison of adiabatic corrections

An important constituent of our models is adiabatic corrections for the tidal shock effects (eqs. 6–8). Various corrections predict different impact of shocks in the middle parts of clusters and lead to different evolutionary paths. The amplitude of the corrections depend on the ratio of the perturbation timescale to the dynamical time of stars in the cluster. For NGC 6254, the characteristic time for disk shocking (eq. [3]) is $\tau_{\text{disk}} = 1.3 \times 10^6$ yr, and for bulge shocking (cf. Gnedin, Hernquist, & Ostriker 1998) is $\tau_{\text{bulge}} = 1.3 \times 10^7$ yr. The half-mass dynamical time of the cluster is initially much shorter, $\omega_h^{-1} = 3.1 \times 10^5$ yr, leading to strong suppression of the effects of tidal shocks.

Figure 9 compares the Spitzer, Weinberg, and N-body adiabatic corrections for the *case 3* models of NGC 6254. When the shocks are “slow” ($x = \omega_h \tau \gg 1$), as indicated by the true values of τ_{disk} and τ_{bulge} , both *S1* and *N1* models have tidal shock effects suppressed more strongly than does *W1* model with less steep adiabatic corrections. For the “slow” shocks, *W1* model gives the correct description of the cluster evolution.

When we decrease the shock timescales by a factor of five, we enter the regime of “fast shocks” and *N2* model is correct. For $x \lesssim 1$, we can estimate the importance of the adiabatic corrections by Taylor expanding equations (6–8). *N2* model shows the slowest evolution because $A_{1N} \approx 1 - 2.5x^2$, whereas for *W2* model, $A_W \approx 1 - 1.5x^2$. Even though the first order correction for *S2* model, $A_{1S} \approx 1 - 2x^2$, is smaller than A_W , the second order correction is larger, $A_{2S} \approx 1 - 1.1x^2$. This allows *S2* model to evolve faster than the others.

Finally, when we reduce the shock timescales by a factor of hundred, the impulse approximation applies everywhere in the cluster and all three models are essentially identical. The evolution in this case proceeds much faster: the cluster is destroyed in half the time of the original model *W1*. Thus, adiabatic corrections are critical for calculating correct globular cluster models.

4.1.2. Low concentration model

For comparison, we consider another model for NGC 6254, with lower concentration $c = 0.84$, or $W_0 = 4$. This is the model used for N-body simulations of Gnedin & Ostriker (1998). All other parameters are the same as in the previous model. We keep the observed tidal radius in parsecs, so the core radius and the relaxation time scale in physical units accordingly (see Table 1).

Figure 10 shows the mass evolution of the low concentration model. The cluster evaporates much faster than the high concentration model, in units of the initial relaxation time $t_{rh,0}$. Clearly, tidal shocks have much stronger effect on less concentrated clusters but the total speed-up in time to destruction, due to shocks, is again about 25%. Figure 11 shows that the evolution of the central density is qualitatively similar to the previous model.

4.2. Multi-mass models

In a single mass model, energy is transferred between the cluster core and the envelope, which requires a conduction mechanism acting on a half-mass relaxation time scale. In a multi-mass model, the energy exchange occurs also between stars of different mass. A typical time scale for energy exchange between the

two mass species m_1 and m_2 ($m_2 < m_1$) is $t_{rh} \times m_2/m_1$. Since this is much shorter than the core collapse time for single mass clusters, the overall evolution of multi-mass clusters is expected to be faster.

Lee & Goodman (1995), for example, considered the evaporation of a multi-mass cluster in a steady tidal field and found that the mass loss rate can more than double relative to the single-component case. Chernoff & Weinberg (1990) investigated the effects of stellar evolution on cluster dynamics. In the future, it will be important to generalize the present calculations by including a realistic mass function and stellar evolution, along with the presently implemented two-body relaxation and tidal shocks. In this paper, we present only an illustrative model allowing for the mass spectrum.

We take the previously described model for NGC 6254 and include seven mass components, ranging from $0.1M_\odot$ to $0.7M_\odot$. The number of stars in each component $N(m) \propto m^{-2}$. Thus, the upper mass limit corresponds to the turn-off of the main sequence at 10 billion years (we also used it in the single-mass models), and the lower limit is a reasonable cutoff of the initial mass function. The relaxation time is defined by equation (21), where we substitute for m_* the mean stellar mass (Lee & Goodman 1995).

Figure 12 shows the mass loss for the multi-mass model. Notice that although the evolution proceeds faster in units of the initial half-mass relaxation time, this timescale expressed in years is longer than that for the single-component model (Table 1). As a result, the destruction time is roughly 20 Gyr in both cases. The contribution of tidal shocks in the multi-mass model is greater, reducing the time to destruction by about 37%.

4.2.1. Comparison with N-body

Recent preprint by Takahashi & Portegies Zwart (1998) compares the multi-mass two-dimensional Fokker-Planck models of Takahashi (1997) with N-body simulations using special purpose computer, *GRAPE-4*. The models include stellar evolution, two-body relaxation, and tidal truncation for a low concentration ($c = 0.67$) cluster from Chernoff & Weinberg (1990). The authors argue that the escape of stars through the tidal boundary in an isotropic F-P code, where the distribution function depends only on energy, E , is faster than in the N-body models. To remedy this disagreement, they suggest a new escape criterion, possible only in an anisotropic F-P code of Takahashi (1995) which follows both energy and angular momentum of stars.

To check that our code does not underestimate the time to destruction, we constructed a *case 0* model of the cluster using the parameters specified in Chernoff & Weinberg (1990). We use 14 mass components from $0.4M_\odot$ to $15M_\odot$, distributed according to the following mass function, $N(m) \propto m^{-2.5}$. Since our model does not include stellar evolution, the time to destruction should be slightly longer than in N-body and 2D F-P models, with give $t_d \approx 1.3t_{rh,0}$. Indeed, we find that our model evolves somewhat slower, with $t_d \approx 2t_{rh,0}$. This allows us to conclude that our results represent an upper limit on the destruction times of globular clusters.

5. Review of Globular Cluster Evolution Including Tidal Shocks

The evolution of the isolated single-mass King models (in dimensionless units) is determined by the only parameter, the concentration c . Inclusion of tidal shocks introduces another independent parameter,

for example, the ratio of the half-mass relaxation time to the characteristic shocking time,

$$\beta \equiv t_{rh}/t_{sh}. \quad (24)$$

The parameter β is a combination of two variables describing the structure of clusters: the number of stars, N , and the mean density, $\rho_h \propto M/R_h^3$. When the amplitude of the tidal force on the cluster is fixed, the tidal shock time (eq. [10]) scales as $t_{sh} \propto \rho_h$, and the relaxation time (eq. [21]) scales as $t_{rh} \propto \rho_h^{-1/2} N / \ln \Lambda$, where $\Lambda = 0.4N$. Then

$$\beta \propto \frac{N}{\ln \Lambda} \rho_h^{-3/2}. \quad (25)$$

While the concentration c describes the effects of two-body relaxation, the parameter β shows the relative importance of tidal shocks. In this Section, we explore the evolution of globular clusters for a wide range of initial parameters c and β .

All the models in this section include full relaxation and tidal shock effects (i.e., *case 3*). We use the adiabatic corrections from N-body simulations for “slow shocks”, equation (7). We arrange a grid of initial conditions, covering a number of cluster concentrations, from $c = 0.6$ to $c = 2.6$ with the step 0.2, and a range of shock parameters, β . We compute 15 models per concentration family, equally spaced on the logarithmic scale from $\beta \approx 10^{-5}$ to $\beta \approx 10^2$. All other parameters correspond to the model of NGC 6254 described in the previous section. The observed tidal radius of NGC 6254 is fixed and the core radius scales accordingly with the concentration.

5.1. Cluster evolution in figures

Figure 13 shows how different regimes of cluster evolution map on the plane of parameters c and β . In the lower left region of the plot tidal shocks are weak and evolution is dominated by two-body relaxation; in the upper left region core collapse proceeds on a relatively short timescale without affecting most of the cluster; and in the lower right region tidal shocks are strong and cause substantial mass loss before core collapse. The upper right region is never reached in reality because of extremely strong tidal shocks leading to fast destruction of the clusters.

Qualitative evolution in the left region of the plane is characteristic of a tidally-truncated model. As clusters start to collapse, the relaxation time becomes increasingly shorter and the tidal shock time becomes increasingly longer because the mean density ρ_h rises (Figure 14). The mass loss is weak at this stage and the number of stars, N , stays relatively constant. As a result, the parameter β decreases (and moves to the left on the diagram) until the very late stages of core collapse. At that point β freezes and the evolutionary tracks are strictly vertical (the upper part of the diagram). After core collapse, the cluster re-expands and its density slightly falls, moving it to the right on the $c - \beta$ diagram. At some later time, so little mass is left that two-body relaxation speeds up again and drives clusters to complete dissolution.

Figure 15 illustrates the behavior of the parameter β with time. On the low end, all lines scale similarly, following the evolution of the mean density. For large initial values of β , the early mass loss due to shocks is very important. This leads us to investigate the right part of the $c - \beta$ diagram.

The evolution of clusters with strong tidal shocks differs dramatically from the previous case. An early mass loss due to shocks changes the structure of clusters, removing stars from the outer parts and adding energy dispersion in the core. This increases the central and the mean density of the clusters. Both core collapse and final destruction proceed much faster. These effects of tidal shocks leave noticeable ripples in the clusters tracks on the right part of the diagram (Figure 13).

Tidal shocking is rapidly self-limiting. Clusters with large values of β quickly lose mass and evolve to $\beta \lesssim 0.1$. Figure 15 demonstrates that just a first few shocks lower the value of β by several orders of magnitude. Every subsequent tidal shock causes the see-saw variations of the shock parameter, with an increasing amplitude towards the end stage of the evolution when fewer stars are left.

A few clusters in the right part of the $c - \beta$ diagram cross their evolutionary tracks on the way to core collapse. At the time of crossing, at least one of the clusters has already suffered a severe mass loss due to shocks and has a structure significantly deviating from King models. The density profiles of the two clusters are similar within the half-mass radii but depart from each other closer to the tidal radius. Those clusters with higher initial concentration and stronger shocks are more severely truncated than the clusters which started with smaller concentration and weaker shocks. Also, tidal shocks add velocity dispersion in the core and, therefore, raise the central density so that the ratio R_t/R_c , as measured by the concentration c , is the same for both clusters.

At the crossing point, the two parameters, c and β , no longer uniquely specify cluster's future path. A third parameter comes into play as we investigate the thermodynamics of clusters.

5.2. Cluster thermodynamics

From a thermodynamic point of view, we can consider stars as particles of gas. A critical factor determining evolution is the heat flow between the core and the halo of the cluster. The heat in this case is the velocity dispersion of stars, $T \equiv v_m^2$, whose flux is derived in Spitzer (1987, p.68). The amount of heat transported through the cluster per unit time, or the “luminosity”, is $4\pi r^2 F(r)$. The heat conduction facilitates core collapse and proceeds on a relaxation time scale. Let us construct a new dimensionless ratio of the heat transported through the half-mass radius in the relaxation time t_{rh} , to the total reservoir of heat, $T(r_h)$. Neglecting constant factors of order unity, we define the following parameter

$$\gamma \equiv - \left. \frac{d \ln v^2}{d \ln r} \right|_{r_h}, \quad (26)$$

which is essentially a logarithmic gradient of the velocity dispersion. For an isothermal sphere, $\gamma = 0$. In general, for clusters on the way to core collapse, this parameter is positive as the heat is transferred from the kinematically hot core to the cold halo, and grows as core collapse accelerates. On the contrary, tidal shocks try to reverse the heat flow by heating preferentially the outer parts of the cluster. Even though the instantaneous value of γ is determined only by the density structure, its derivative, $\dot{\gamma}$, is a signature of the relaxation- or tidal shock-driven evolution.

The clusters crossing paths on the $c - \beta$ diagram have similar values of γ , but the derivatives have opposite sign. For the clusters moving almost vertically on the diagram, $\dot{\gamma} > 0$, whereas for the clusters which cross the diagram horizontally, $\dot{\gamma} < 0$. Therefore, the evolution of the former is dominated by two-body relaxation and the latter by tidal shocks.

Knowing the value of $\dot{\gamma}$ for Galactic globular clusters, we could in principle differentiate the two evolutionary paths. Unfortunately, it is very hard to establish the sign of $\dot{\gamma}$ observationally.

Another signature of the tidal shock-dominated clusters is a steep density profile and a low number density of stars at the tidal radius. Strong shocks sweep away a large number of stars at once and leave the cluster filling smaller volume in space than is provided by the external tidal field. Clusters with a sharp density contrast and a high velocity dispersion of the halo stars might be experiencing strong shocking.

Most of such clusters are expected to come very close to the Galactic center but are not necessarily present there now.

5.3. Cluster evolution in numbers

The mass loss from clusters is strongly enhanced by tidal shocks. An illustration of this is the fraction of the initial mass remaining at the time of core collapse, $M(t_{cc})$. Figure 16 shows that the larger β , the smaller the remaining mass. Note, that many models of initial various concentration converge at $\beta \approx 0.1$, giving $M(t_{cc}) \approx 45\%$.

The core collapse time is a strong function of both initial parameters c and β . Figure 17 shows t_{cc} for the models without tidal shocks. In units of the initial half-mass relaxation time, the core collapse time can be fitted as follows:

$$\frac{t_{cc}}{t_{rh,0}} = f_1(c) \equiv 10^{a_1 + a_2 c + a_3 c^2 + a_4 c^3 + a_5 c^4}, \quad (27)$$

where the coefficients a_i are given in Table 2. Our results are in good agreement with Quinlan (1996), except for the clusters with very high concentration. Even for them, the maximum difference is less than 30%.

Figure 18 shows the core collapse time for the models including tidal shocks. The shock-induced relaxation speeds up core collapse by adding velocity dispersion in the core and by removing stars in the outer parts of the clusters, thus reducing the relaxation time. We fit the results assuming, as an *Ansatz*, the following functional form:

$$\frac{t_{rh,0}}{t_{cc}} = \frac{t_{rh,0}}{t_{cc}} \Big|_{\beta=0} (1 + b_1 \beta^{b_2} + b_3 \beta^{b_4}). \quad (28)$$

The coefficients b_i for models of various concentration c are given in Table 3. The fit is generally accurate to 20%, with larger errors for models with very high initial concentration.

The time to destruction, t_d , is also strongly affected by tidal shocks. As we have emphasized in the previous section, evolution of clusters with different parameters scales similarly when time is normalized to the core collapse time. Accordingly, we provide the fitting formulae for the scaled destruction time, t_d/t_{cc} . For the models without tidal shocks (Figure 19), we use the same functional form as equation (27) and fit t_d both in units of the initial relaxation time and in units of the core collapse time:

$$\frac{t_d}{t_{rh,0}} = f_2(c), \quad \frac{t_d}{t_{cc}} = f_3(c), \quad (29)$$

where the coefficients a_i are again given in Table 2.

For the models including tidal shocks (Figure 20), the scaled destruction time varies very little for the low concentration clusters and increasingly more for the high concentration ones. Interestingly enough, regardless of the initial structure, models with strong shocks converge to an almost constant value $t_d/t_{cc} \sim 2$. It follows that the core collapse time is a midpoint in cluster's lifetime.

Since the value of t_d/t_{cc} is almost constant for $\beta \ll 1$ and for $\beta \gg 1$, we choose the following functional form to fit the results:

$$\frac{t_d}{t_{cc}} = \frac{t_d}{t_{cc}} \Big|_{\beta=0} \left(\frac{1 + d_1 \beta^{d_2}}{1 + d_3 \beta} \right), \quad (30)$$

where the coefficients a_i are given in Table 4. This expression allows for a variation in the slope of the fit for large values of β , but the coefficient d_2 is always close to unity, as expected.

In the case of very strong shocks, both the core collapse and the destruction times scale approximately as $t_{cc}, t_d \propto \beta^{-1/2}$ (cf. the coefficient b_2 in Table 3). This asymptotic behavior can be understood as follows. The shock parameter β is proportional to the mean energy change due to shocks (eq. [9]), which in turn is proportional to the amplitude of the tidal force squared, I^2 . Therefore, the approximate scaling of t_{cc} and t_d indicate that these timescales vary inversely proportional to I .

6. Discussion

Our Fokker-Planck models provide the most comprehensive calculations of the globular cluster evolution including gravitational tidal shocks. We find that tidal shocks significantly alter the evolution, in agreement with the earlier studies by Spitzer & Chevalier (1973) and more recent ones by Gnedin & Ostriker (1997). Globular clusters appear to be rather fragile with regard to the effects of tidal shocking.

Tidal shocks accelerate dynamical evolution and evaporation of clusters by effectively stripping stars in the outer regions and adding energy dispersion in the core. These effects are self-limiting: as clusters lose mass and become more compact, the relative importance of tidal shocks rapidly diminishes in favor of two-body relaxation.

We examine several types of adiabatic corrections: the harmonic approximation (of L. Spitzer), the linear perturbation theory (of M. Weinberg), and the results of N-body simulations. The differences between the various types of adiabatic corrections depend on the regime of “slow shocks” or “fast shocks”, but overall the corrections are critical for accurate calculation of the evolution. Without adiabatic corrections, the destruction time of NGC 6254 is twice as short.

The evolution of models with a single mass component can be characterized by the King-model concentration parameter, c , and the shock parameter, β (eq. [24]). The effects of tidal shocks are important when $\beta \gtrsim 10^{-3} - 10^{-2}$, depending on the concentration. Tidal shocks increase both the mean and the central densities, relative to the relaxation case. Core collapse is significantly accelerated, and in the limit of strong shocks, the core collapse time scales approximately as $t_{cc} \propto \beta^{-1/2}$. The time to destruction is also dramatically reduced, following the same scaling law. Overall, we find that evolution of models proceeds very similarly when time is expressed in units of the core collapse time. In the limit of strong shocks, the destruction time $t_d \approx 2t_{cc}$, independently on the initial concentration. Core collapse provides a useful midpoint of cluster evolution.

We also consider an illustrative model with a range of stellar masses. In units of the initial relaxation time, the evolution proceeds much faster than in the single-mass case, but for both models the time to destruction is comparable when expressed in years. A systematic study of multi-mass models is beyond the scope of the present study and requires a knowledge of the initial mass function in star clusters.

The results of our calculations have important implications for the evolution of globular clusters. Not only will the current population of clusters be significantly depleted in the future (Gnedin & Ostriker 1997), but also a large fraction of the initial population might have been already destroyed in the Galaxy. Since the shock effects quickly saturate, tidal shocks must have been more important in the past.

The current calculations can be improved in several ways. A reasonable mass function and effects of

stellar evolution should be included in order to accurately describe the early phase of cluster evolution. Also, in our treatment of tidal shocks, we have neglected small (but real) negative relaxation due to cluster oscillations. The final weakness of our models is the assumption of the isotropic velocity distribution. Radial anisotropy would develop in the outer parts in the absence of tidal shocks. Since the stars on radial orbits will be ejected more easily than those on circular orbits, tidal shocks should effectively isotropize orbits even in the outer parts. Takahashi (1995,1997) and Takahashi, Lee, & Inagaki (1997) have developed an accurate method for integrating the anisotropic Fokker-Planck equation. We plan to include the effect of tidal shocks in the anisotropic code in order to clarify these points.

We would like to thank Kathryn Johnston for useful discussions. This work was supported in part by NSF grant AST 94-24416 and by Korea Science and Engineering Foundation grant No. 95-0702-01-01-3.

REFERENCES

Aguilar, L., Hut, P., & Ostriker, J. P. 1988, *ApJ*, 335, 720

Allen, C., & Santillan, A. 1991, *RMxAA*, 22, 255

Ambartsumian, V. A. 1938, *Uch. Zap. L.G.U.*, 22, 19. English transl. in IAU Symposium 113, *Dynamics of Star Clusters*, ed. J. Goodman, & P. Hut (Dordrecht: Reidel), 521

Antonov, V. A., 1962, *Vestnik Leningrad Univ.*, 7, 135. English transl. in IAU Symp. No. 113, *Dynamics of Star Clusters*, ed. J. Goodman, & P. Hut (Dordrecht: Reidel), 525

Chernoff, D. F., & Shapiro, S. L. 1987, *ApJ*, 322, 113

Chernoff, D. F., & Weinberg, M. D. 1990, *ApJ*, 351, 121

Cohn, H. N. 1979, *ApJ*, 234, 1036

Cohn, H. N. 1980, *ApJ*, 242, 765

Cohn, H. N. 1985, in *Dynamics of Star Clusters*, IAU Symposium 113, ed. J. Goodman, & P. Hut (Dordrecht: Reidel), 161

Gnedin, O. Y., Hernquist, L., & Ostriker, J. P. 1998, *ApJ*, submitted; [astro-ph/9709161](http://arxiv.org/abs/astro-ph/9709161)

Gnedin, O. Y., & Ostriker, J. P. 1997, *ApJ*, 474, 223

Gnedin, O. Y., & Ostriker, J. P. 1998, *ApJ*, submitted

Goodman, J. 1993, in *Structure and Dynamics of Globular Clusters*, ASP Conf. Ser., vol. 50, ed. S. G. Djorgovski, & G. Meylan (San Francisco: ASP), 87

Hénon, M. 1961, *Ann. d'Ap.*, 24, 369

Johnston, K. V., Hernquist, L., & Weinberg, M. 1998, *ApJ*, submitted

Kim, S. S., Lee, H. M., & Goodman, J., 1998, *ApJ*, 495, 786

King, I. R. 1966, *AJ*, 71, 64

Kundić, T., & Ostriker, J. P., 1994, *ApJ*, 438, 702

Lee, H. M., 1987, *ApJ*, 319, 801.

Lee, H. M., & Goodman, J. 1995, *ApJ*, 443, 109

Lee, H. M., & Ostriker, J. P. 1987, *ApJ*, 322, 123

Lee, H. M., & Ostriker, J. P. 1993, *ApJ*, 409, 617

Lee, H. M., Fahlman, G. G., & Richer, H. B. 1991, *ApJ*, 366, 455

Lynden-Bell, D. & Wood, R., 1968, *MNRAS*, 138, 495.

Odenkirchen, M., Brosche, P., Geffert, M., & Tucholke, H.-J. 1997, *New Astronomy*, 2, 477

Oh, K. S., & Lin, D. N. C., 1992, *ApJ*, 386, 519.

Ostriker, J. P. 1985, in *Dynamics of Star Clusters*, IAU Symposium 113, ed. J. Goodman, & P. Hut (Dordrecht: Reidel), 347

Ostriker, J. P., Spitzer, L. Jr., & Chevalier, R. A. 1972, *ApJ*, 176, L51

Quinlan, G. D. 1996, *New Astronomy*, 1, 255

Spitzer, L. Jr. 1940, *MNRAS*, 100, 397

Spitzer, L. Jr. 1987, *Dynamical Evolution of Globular Clusters* (Princeton: Princeton Univ. Press)

Spitzer, L. Jr., & Chevalier, R. A. 1973, *ApJ*, 183, 565

Spitzer, L. Jr., & Hart, M. H. 1971, *ApJ*, 164, 399

Takahashi, K., 1995, *PASJ*, 47, 561

Takahashi, K., 1997, *PASJ*, 49, 547

Takahashi, K., Lee, H. M., & Inagaki, S. 1997, *MNRAS*, 292, 331

Takahashi, K., & Portegies Zwart, S. F. 1998, [astro-ph/9805310](#)

Weinberg, M. D., 1994, *AJ*, 108, 1398; 1403; 1414.

Table 1. Model parameters for NGC 6254.

Model	c	$t_{rh,0}$ (Gyr)	$t_{sh}/t_{rh,0}$	$t_{cc}/t_{rh,0}$	$t_d/t_{rh,0}$
SINGLE MASS	1.4	0.76	96		
<i>case 0</i>				12.9	32
<i>case 1</i>				10.0	26
<i>case 2</i>				11.2	32
<i>case 3</i>				9.7	24
LOW CONCENTRATION	0.84	1.80	7.3		
<i>case 0</i>				12.2	16.5
<i>case 1</i>				8.0	13.5
<i>case 2</i>				8.5	14.5
<i>case 3</i>				7.1	12
MULTI-MASS	1.4	2.77	15		
<i>case 0</i>				1.76	13.5
<i>case 1</i>				1.59	9.5
<i>case 2</i>				1.60	13
<i>case 3</i>				1.57	8.5

Table 2. Fitting coefficients for t_{cc} and t_d versus c .

Function	a_1	a_2	a_3	a_4	a_5
$f_1(c)$	1.3162	-1.9809	3.2910	-1.8401	0.2987
$f_2(c)$	1.2897	-1.1223	1.9824	-0.8803	0.1104
$f_3(c)$	0.1286	0.3173	-0.6573	0.6367	-0.1319

Table 3. Fitting coefficients for t_{cc} versus β .

c	b_1	b_2	b_3	b_4
0.8	1.5029	0.5539	0.0185	0.4558
1.0	0.1174	1.4184	1.6004	0.4491
1.2	0.5124	0.8597	1.5189	0.3840
1.4	3.3268	0.4680	-1.0819	0.5281
1.6	2.9924	0.4613	-1.0366	0.5726
1.8	1.1447	0.3691	0.1791	0.3614
2.0	1.4912	0.2996	-0.7153	0.1606
2.2	0.8931	0.6518	-0.6721	0.2626
2.4	0.6413	0.5716	-0.9622	0.2167
2.6	0.9452	0.5916	-1.4586	0.2065

Table 4. Fitting coefficients for t_d versus β .

c	d_1	d_2	d_3
0.8	2.1942	1.0376	2.3645
1.0	0.1315	1.2982	0.2646
1.2	1.6051	1.1528	2.6816
1.4	45.420	1.0356	74.731
1.6	135.52	0.9993	300.84
1.8	188.62	0.9932	587.29
2.0	159.24	0.9675	788.60
2.2	83.444	0.9608	667.98
2.4	40.040	1.0309	520.84
2.6	42.112	1.1056	862.75

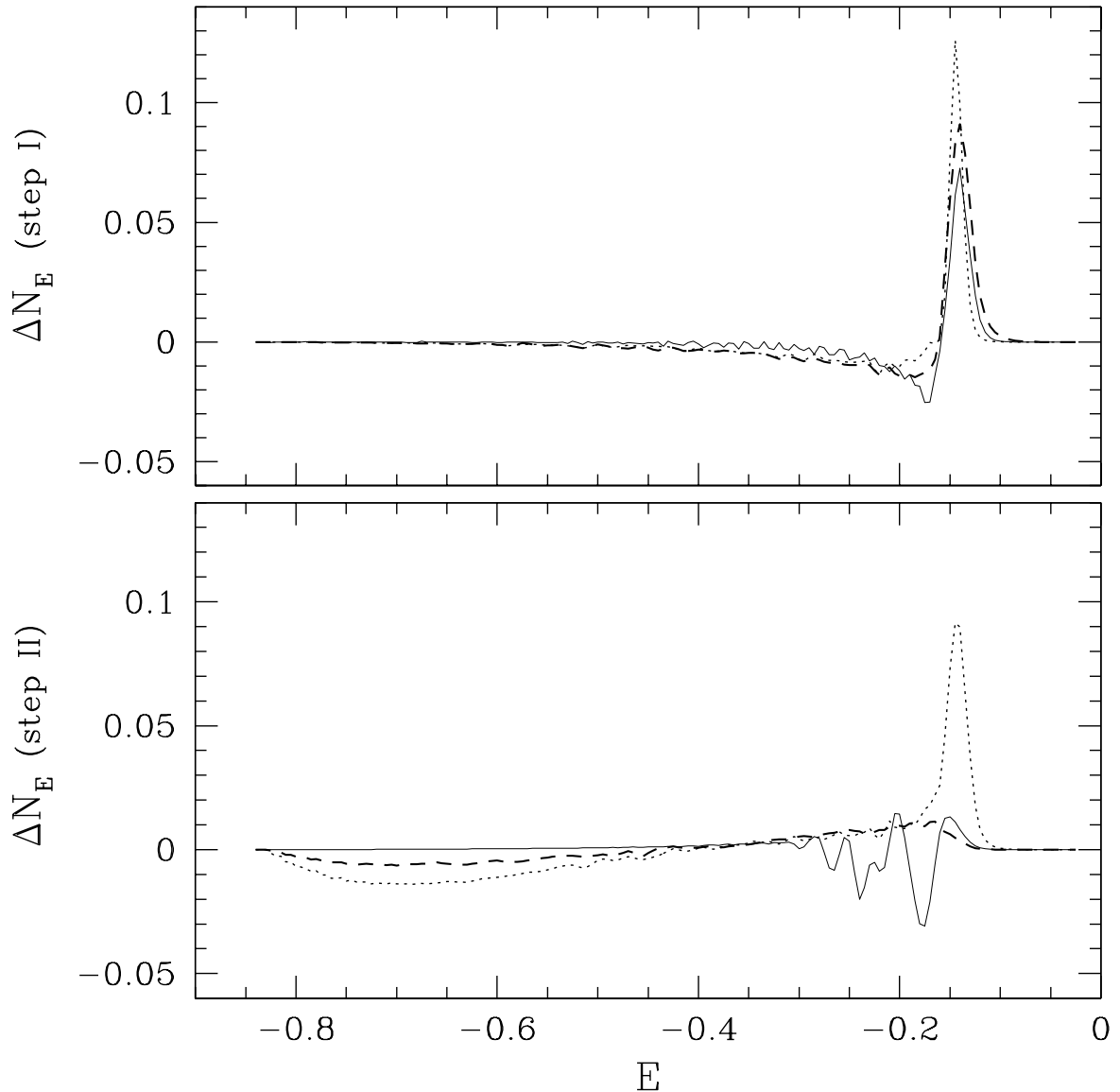


Fig. 1.— Comparison of the energy density change, $\Delta N(E)$, for the current Fokker-Planck (dashes) and N-body calculations (solid lines). Energy on the horizontal axis is normalized to the cluster binding energy. The test cluster is initially a King model with the concentration $c = 0.84$. A single weak shock is applied, similar to the ones studied by Gnedin & Ostriker (1998). Dots show previous implementation of tidal shocks in the F-P code, where the distribution function was kept fixed as a function of adiabatic invariants. The current procedure agrees with N-body results much more accurately, especially in the center and the outer parts of the cluster.

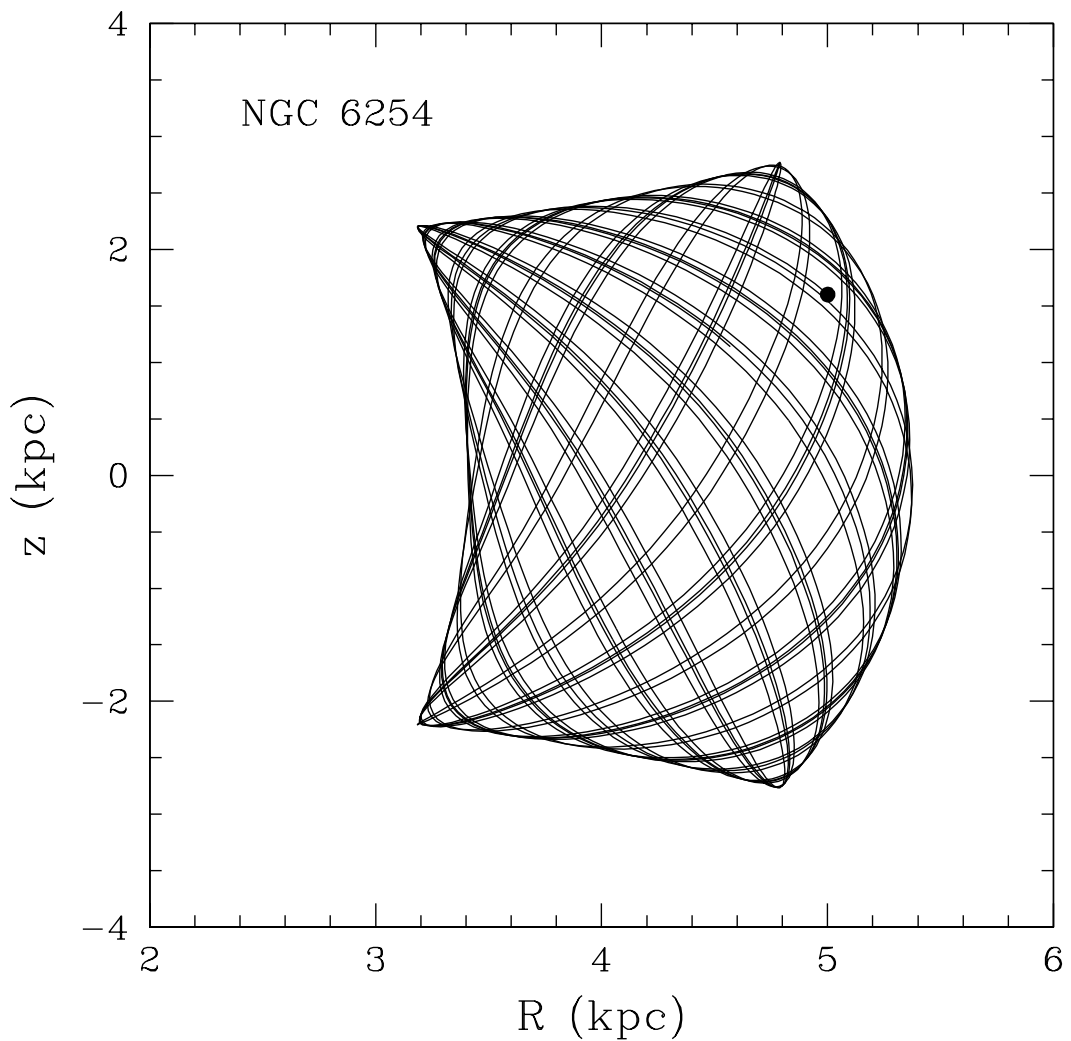


Fig. 2.— Orbits of NGC 6254 in the analytic potential of the Galaxy from Allen & Santillan (1991), for 3×10^9 years. The dot marks the current position of the cluster.

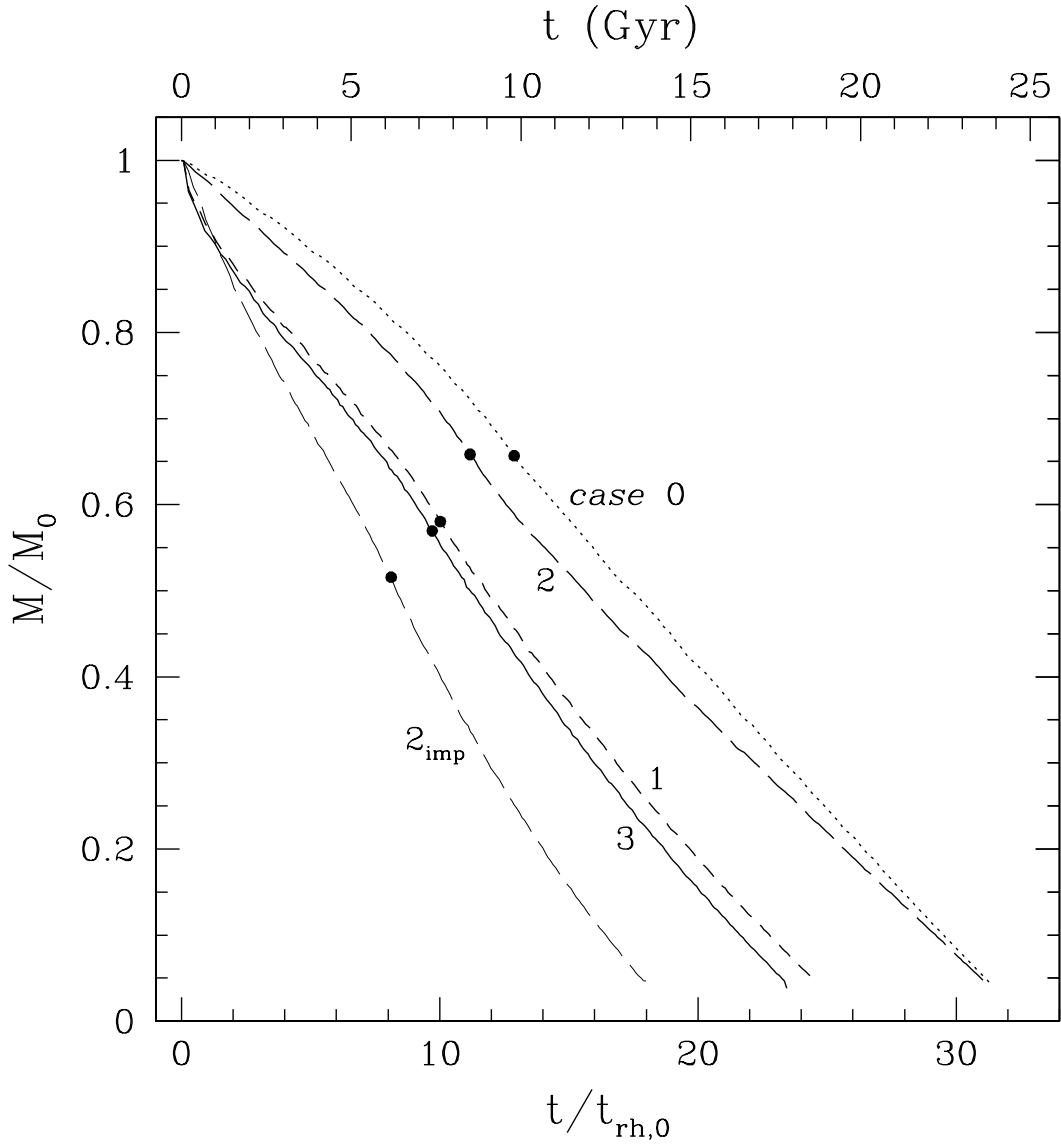


Fig. 3.— Mass loss for single-mass models of the globular cluster NGC 6254. Time is expressed in units of the initial half-mass relaxation time, as well as in billions of years. Dots are for the model with two-body relaxation only (*case 0*), dashes are for the model that includes the effects of the energy shift due to tidal shocks (*case 1*), long dashes are for the model that includes the second order energy dispersion (without the heating term; *case 2*), and solid line is for the final model including proper treatment of all of the shock effects (*case 3*). The adiabatic corrections for “slow shocks” from N-body simulations are used (eq. [7]). Thin dashes show the effect of the second order term (ϱ_{imp}) if it had not had adiabatic corrections. Filled circles indicate the time of maximum core collapse.

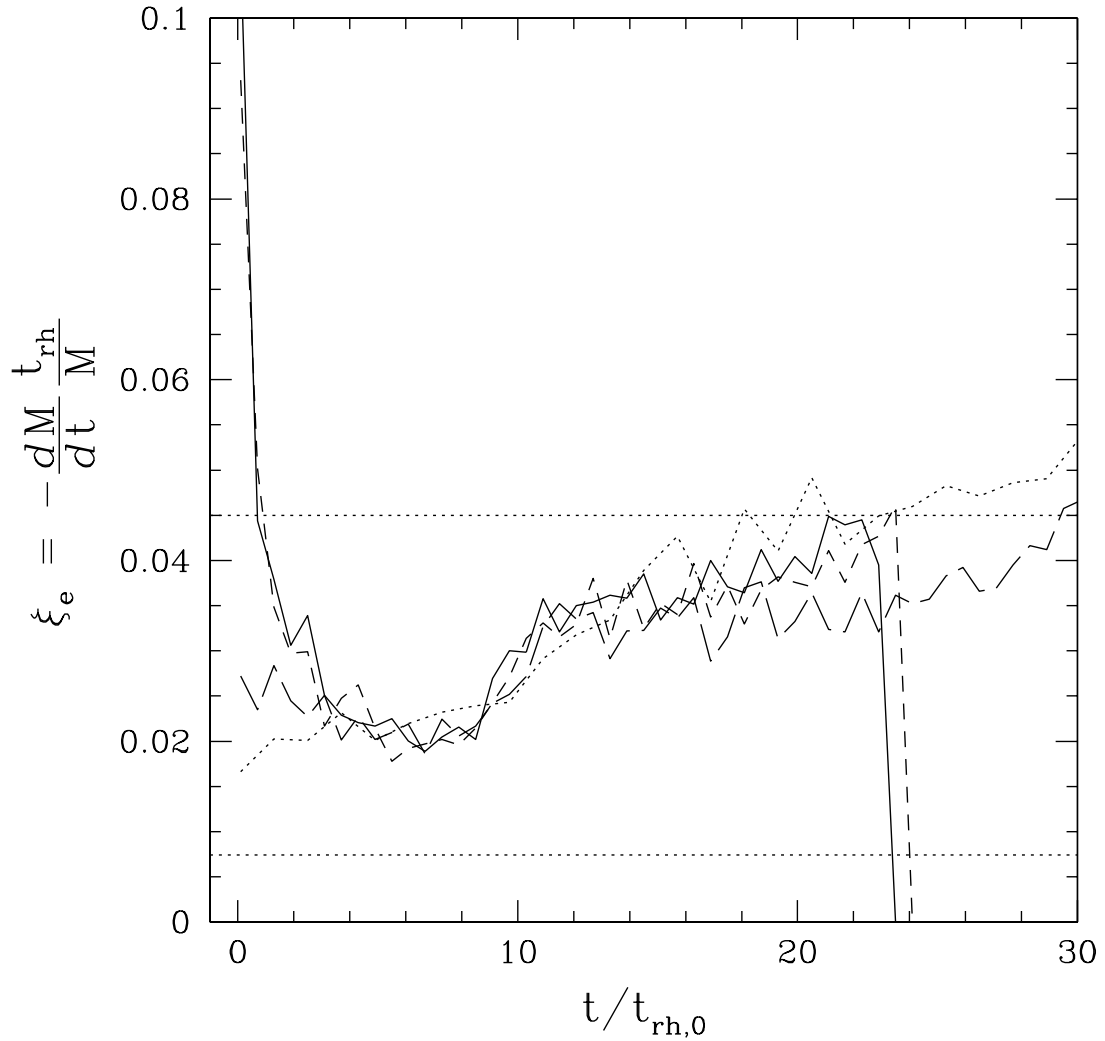


Fig. 4.— Escape probability in units of the half-mass relaxation time for NGC 6254. Line notation is the same as in Fig. 3. Lower horizontal line shows analytical estimate by Ambartsumian (1938), $\xi_e = 0.0074$, and upper self-similar calculations by Hénon (1961), $\xi_e = 0.045$.

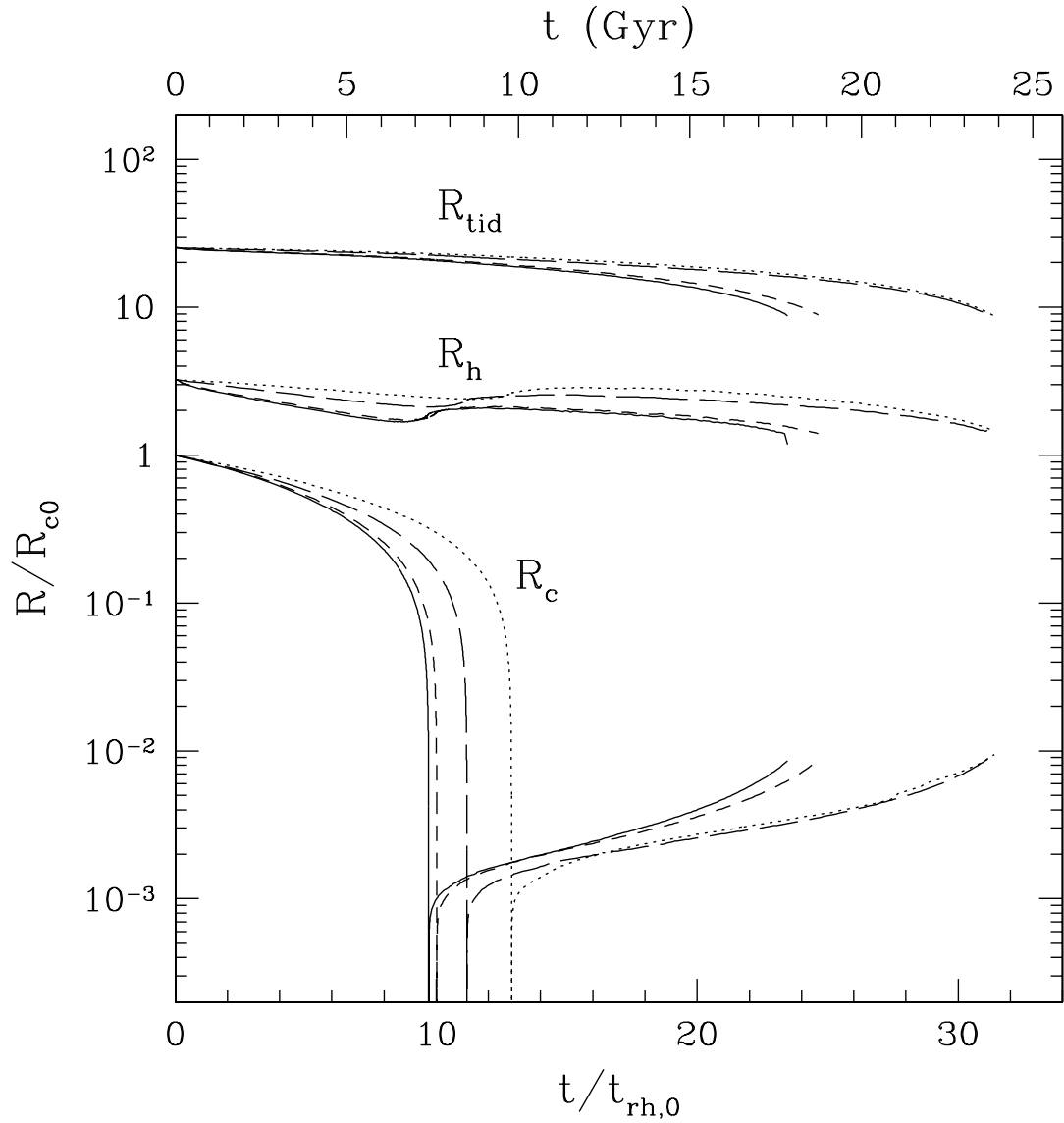


Fig. 5.— Evolution of the tidal, half-mass, and core radii of NGC 6254. Line notation is the same as in Fig. 3.

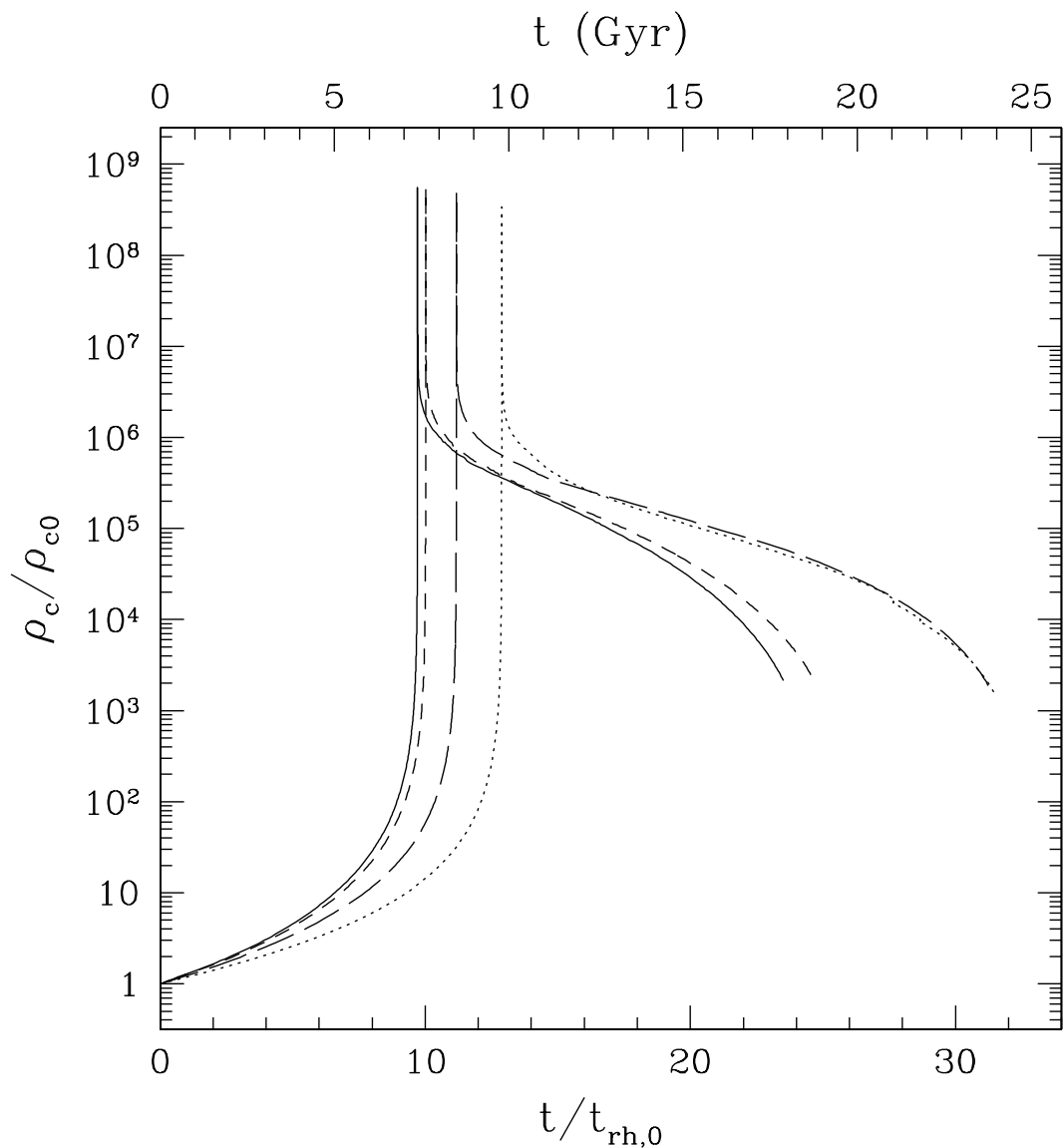


Fig. 6.— Evolution of the central density of NGC 6254. Line notation is the same as in Fig. 3.

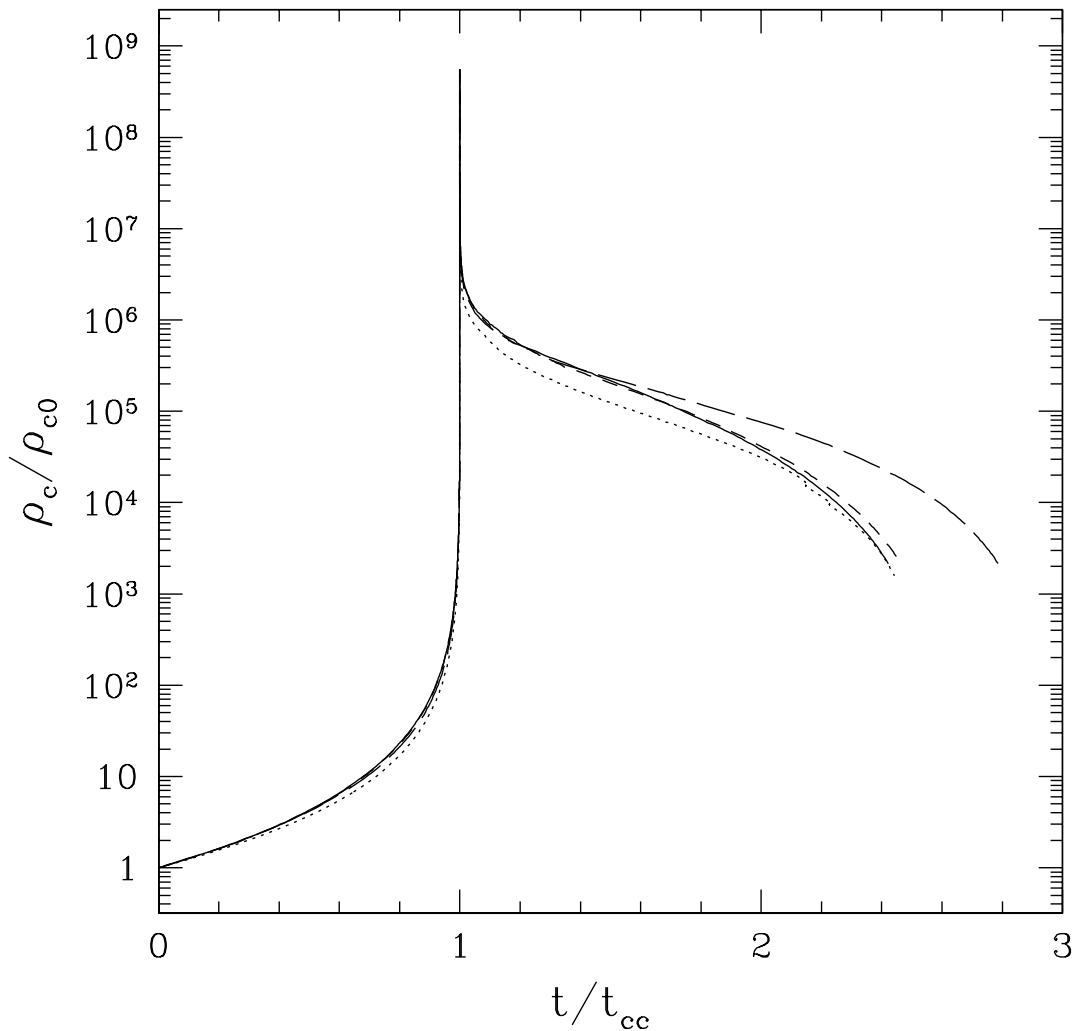


Fig. 7.— Central density of NGC 6254 in the units of time scaled to the individual core collapse times. Evolution in these scaled units is similar for all models. Line notation is the same as in Fig. 3.

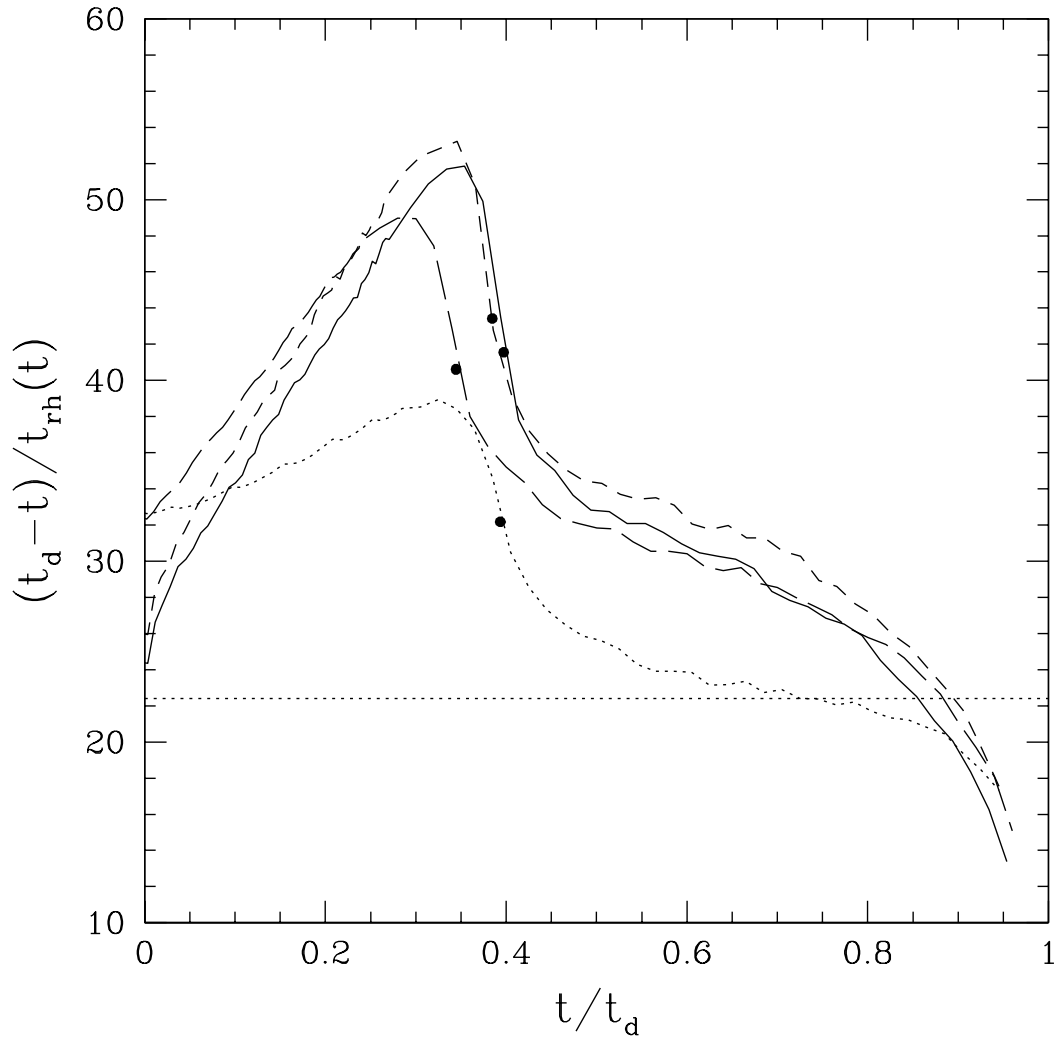


Fig. 8.— Time to destruction of the cluster NGC 6254 in units of the current relaxation time, $t_{rh}(t)$, versus cluster age. Line notation is the same as in Fig. 3. The filled circles indicate the time of maximum core collapse. The dotted horizontal line is Hénon's self-similar solution, equation (23). Time is normalized to the different destruction time t_d for each model.

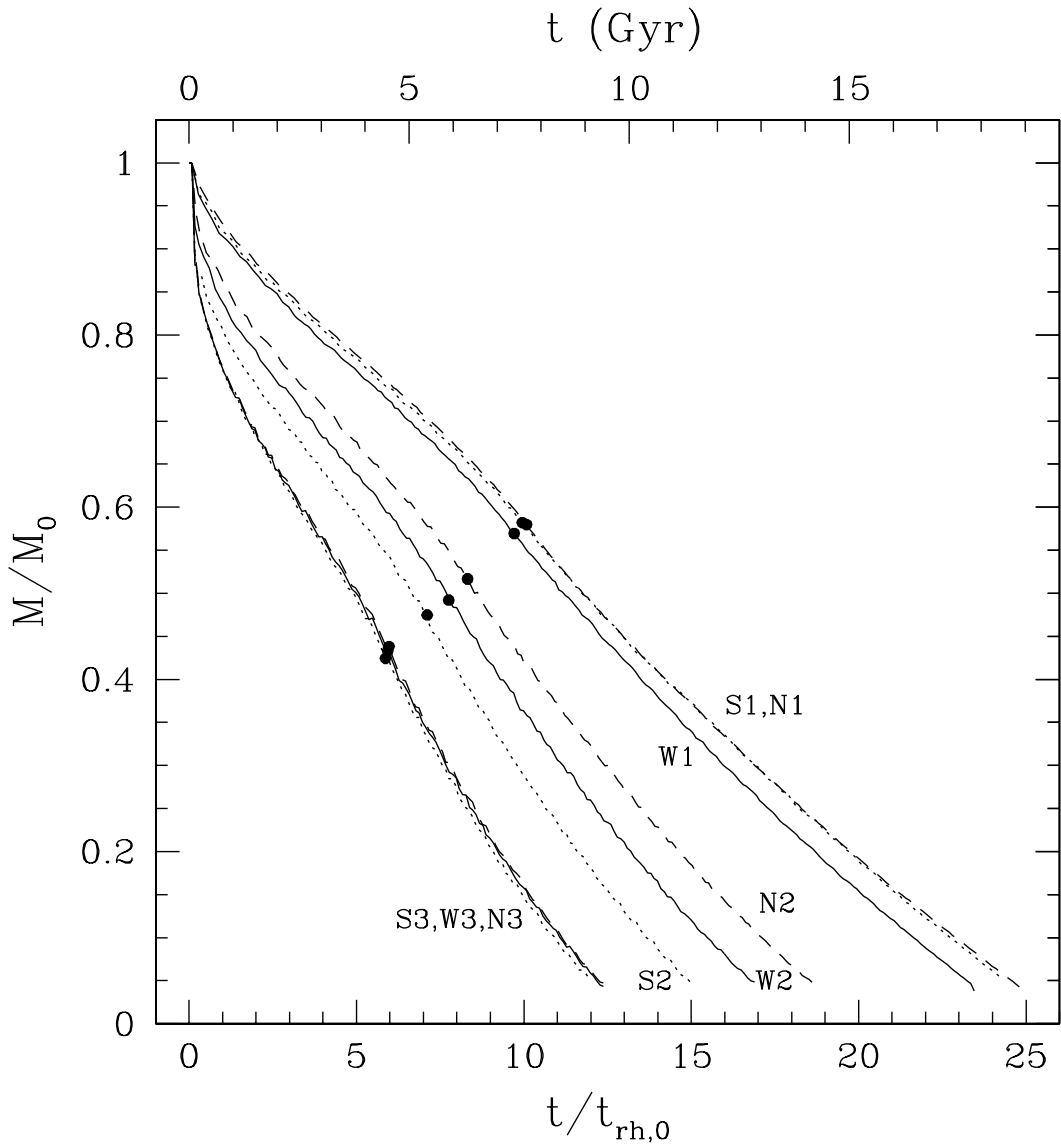


Fig. 9.— Comparison of the Spitzer (S), Weinberg (W), and N-body (N) adiabatic corrections for the *case 3* models of NGC 6254. The first set of models ($S1, W1, N1$) is calculated with the actual values of the disk and bulge shock timescales, τ_{disk} and τ_{bulge} ; the second set ($S2, W2, N2$) with the shock timescales reduced by a factor of 5; and the third set ($S3, W3, N3$) with the shock timescales reduced by a factor of 100. Solid lines correspond to the Weinberg corrections (eq. [7]), dots to the Spitzer corrections (eq. [6]), and dashes to the N-body corrections for fast shocks (eq. [8]). Filled circles indicate the time of maximum core collapse.

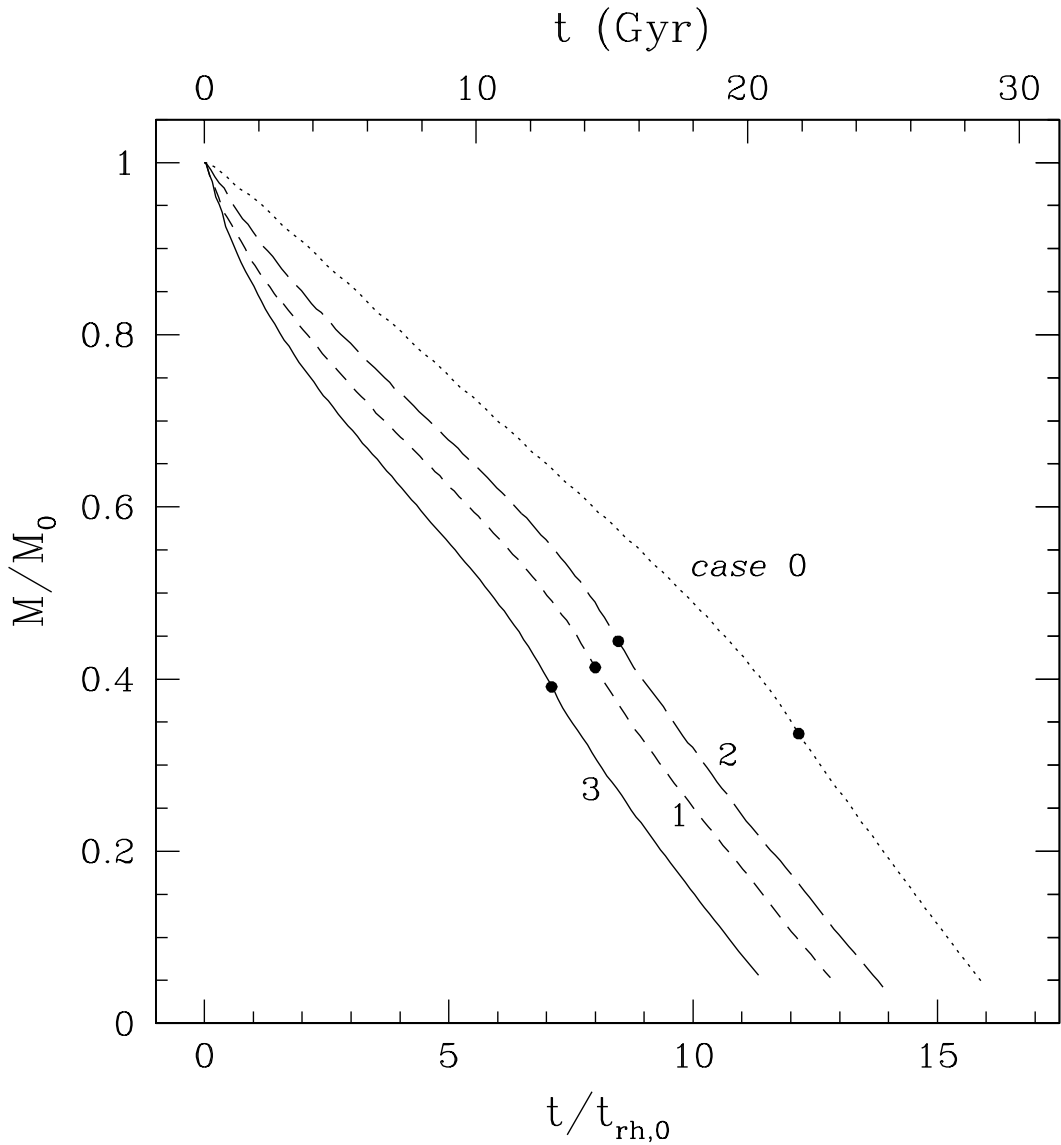


Fig. 10.— Mass loss of the low concentration model, $c=0.84$. All other parameters of NGC 6254 are fixed, including the tidal radius in parsecs. Line notation is the same as in Fig. 3.

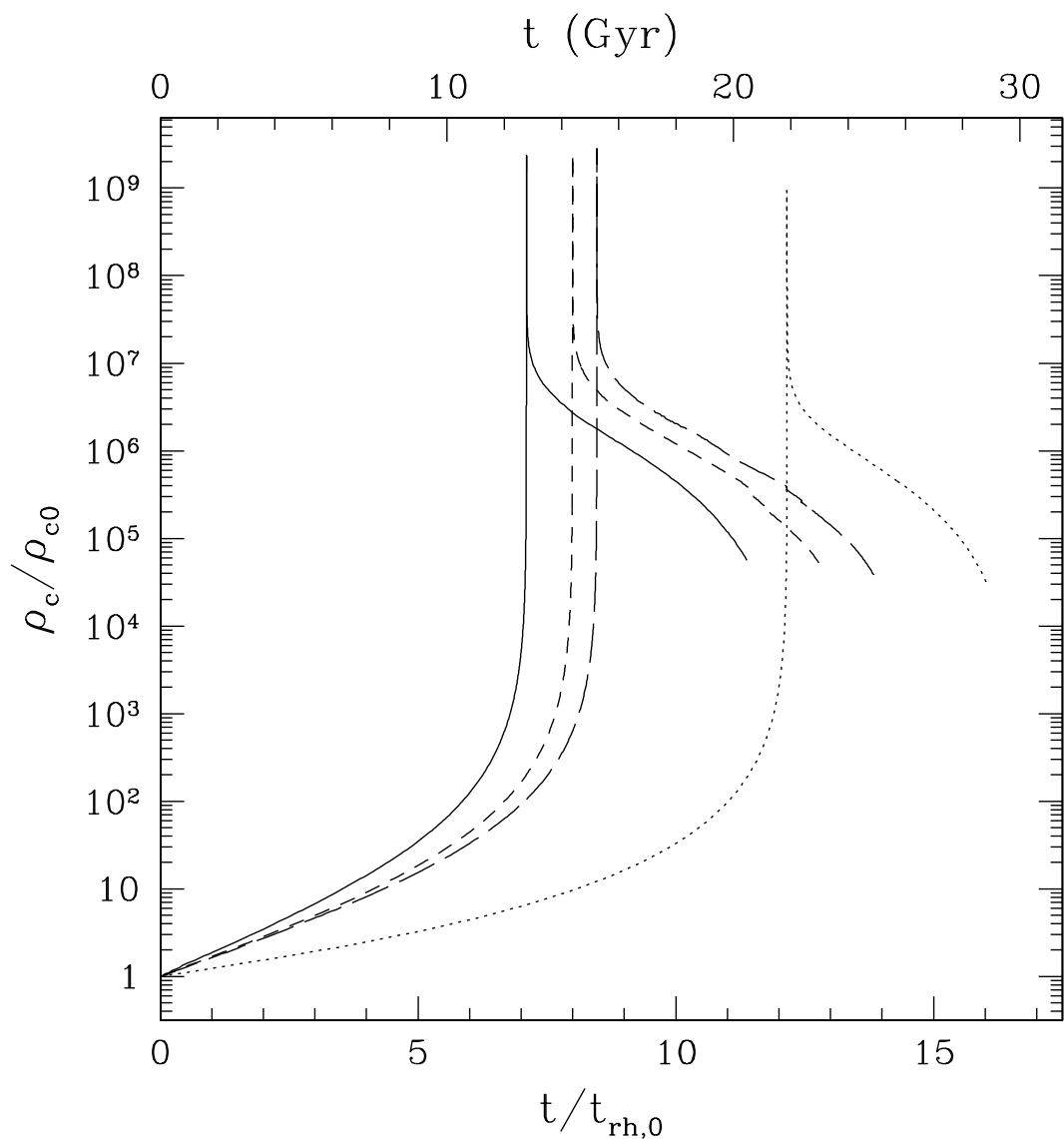


Fig. 11.— Central density of the low concentration cluster. Line notation is the same as in Fig. 3.

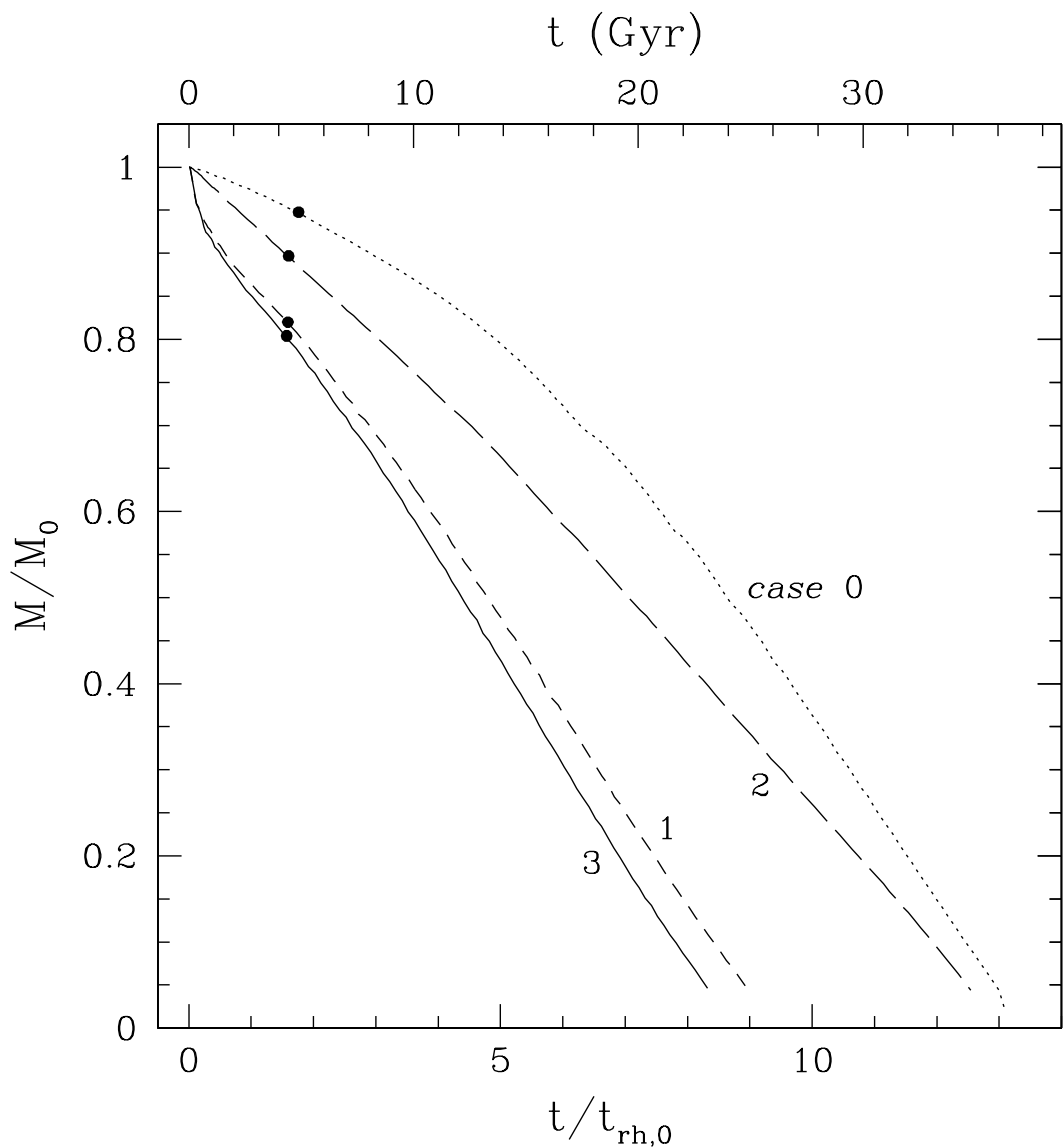


Fig. 12.— Mass loss of the multi-mass model of NGC 6254. Line notation is the same as in Fig. 3.

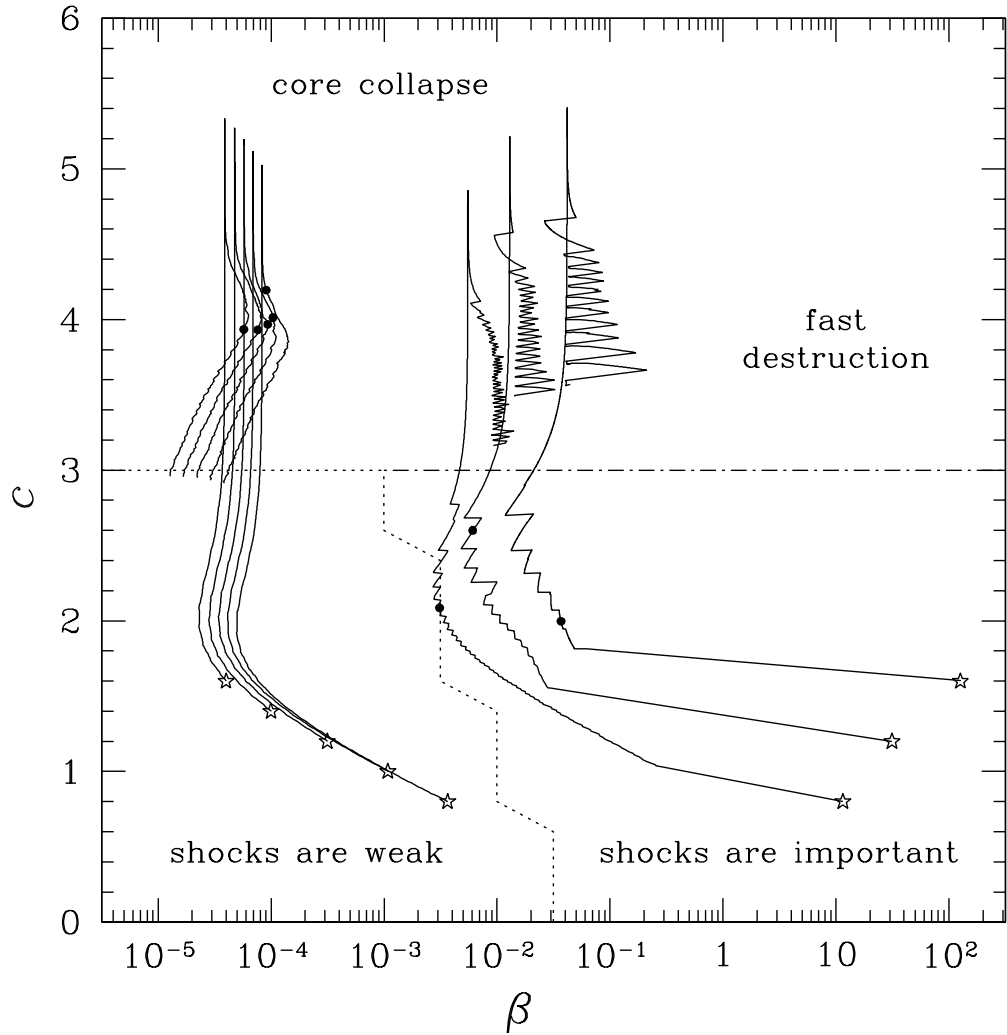


Fig. 13.— Evolution of model clusters as a function of the concentration, c , and the shock parameter, β . Stars show the initial conditions, filled circles the time of core collapse. Marked regions on the diagram correspond to different regimes of cluster evolution. The critical values of β , separating the left and right regions, are determined when the core collapse time deviates from its value for $\beta = 0$.

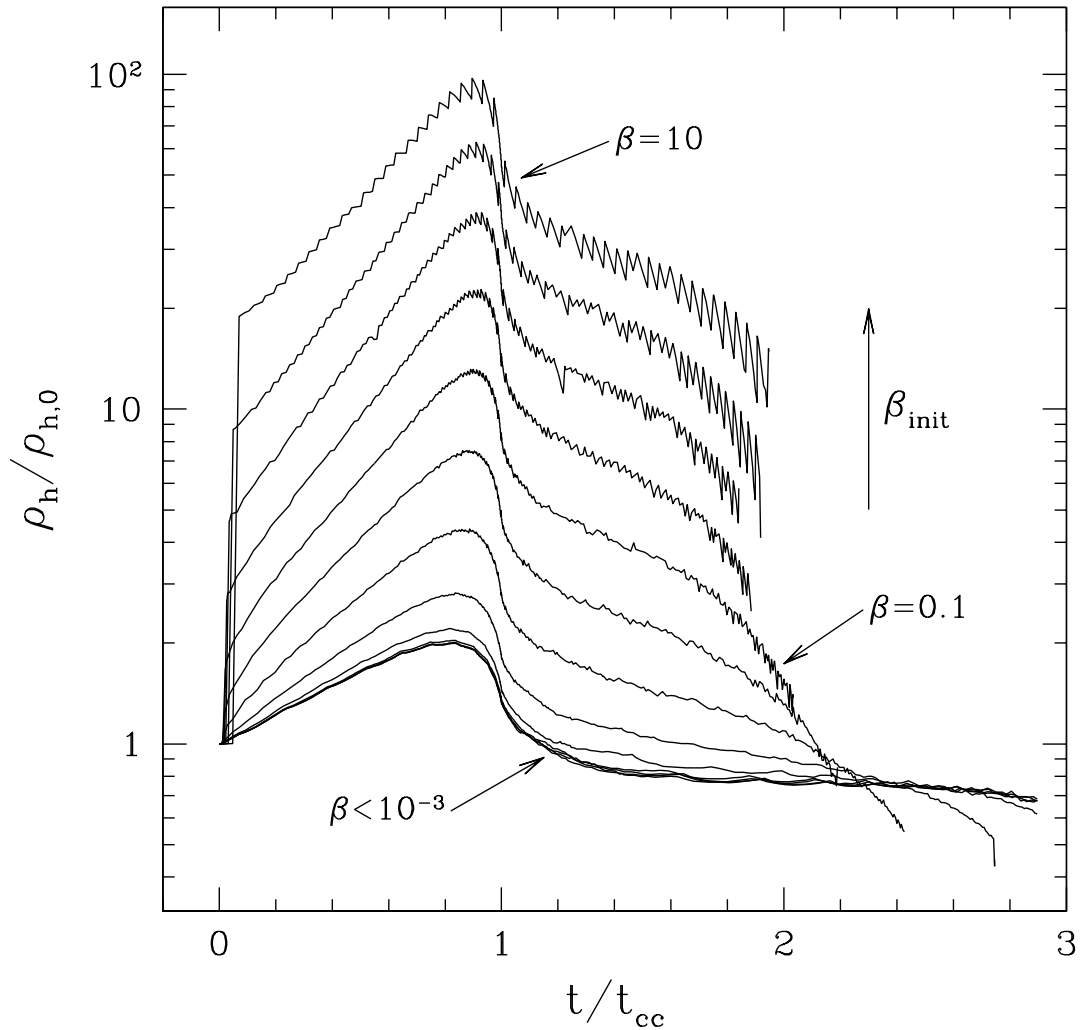


Fig. 14.— The mean density, ρ_h , as a function of time normalized to the individual core collapse time for each run. All models shown have the same initial concentration $c = 1.4$, but different shock parameters varying from $\beta = 10^{-5}$ to $\beta = 10$. Models with $\beta < 10^{-3}$ show essentially identical evolution. At the time of core collapse, the mean density is higher for the higher values of β .

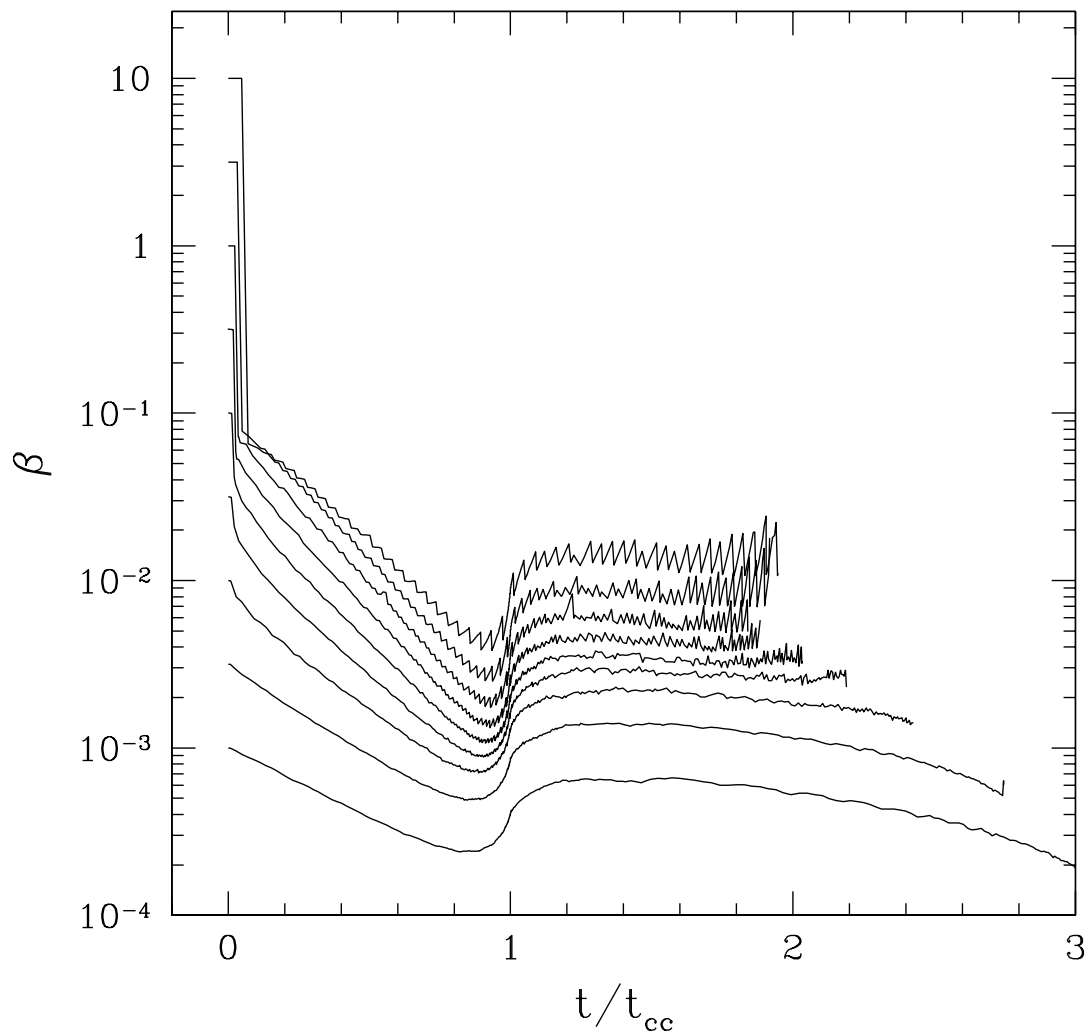


Fig. 15.— The shock parameter, β , as a function of time normalized to the individual core collapse time, for models with various initial values of β and the same initial concentration $c = 1.4$.

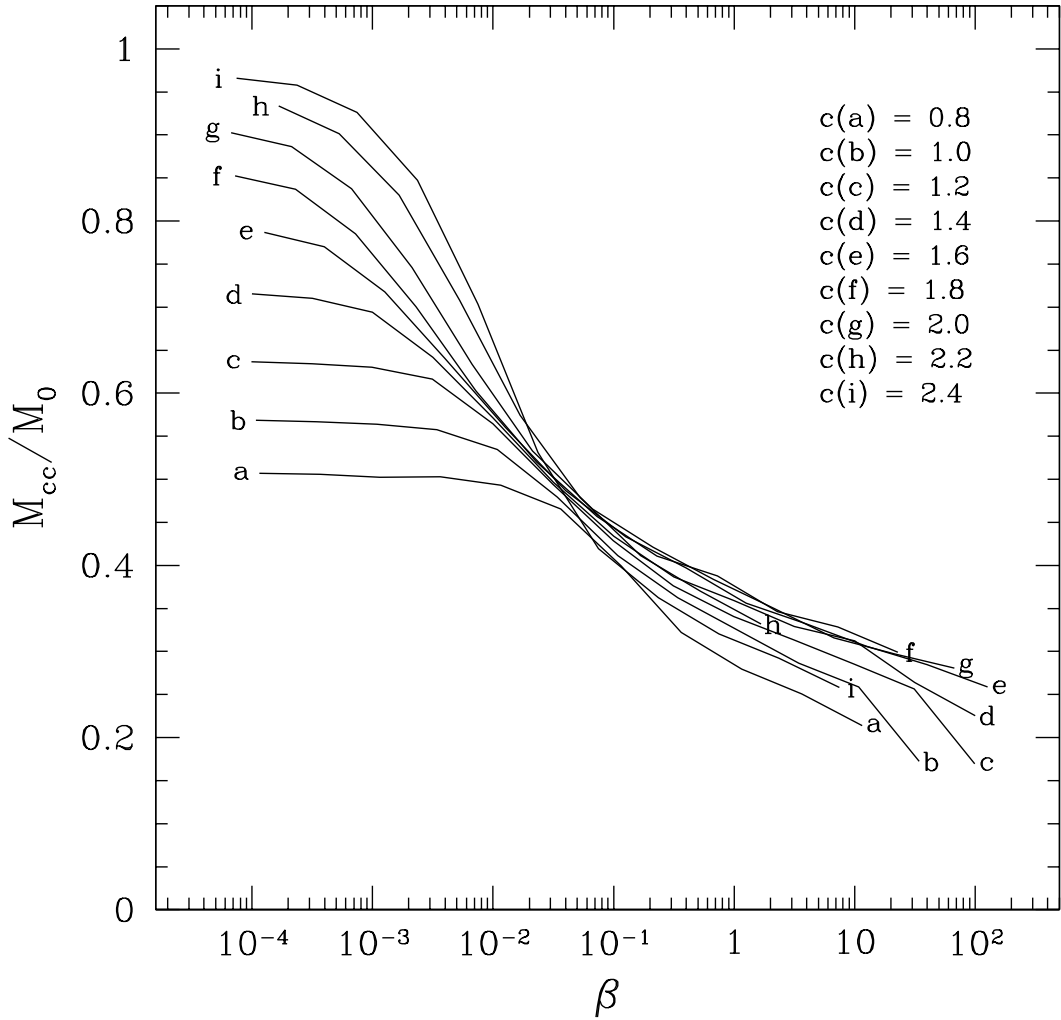


Fig. 16.— The mass remaining at the time of core collapse versus the shock parameter, β , for various families of cluster models. Each family has the same initial concentration, from $c = 0.8$ for family a to $c = 2.4$ for family i . Letters correspond to the end models of each family.

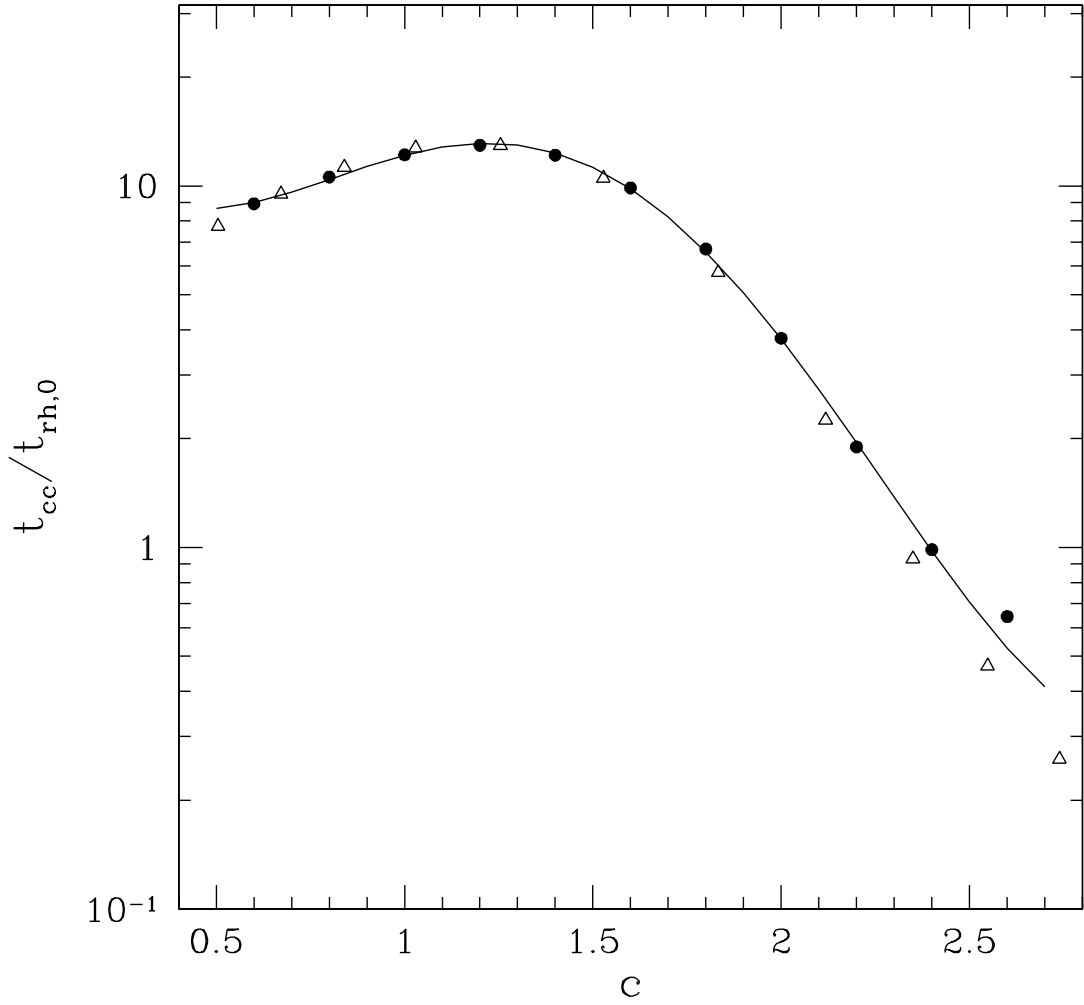


Fig. 17.— The core collapse time as a function of the initial concentration for the models without tidal shocks. Filled dots are our results, triangles are from Quinlan (1996). The agreement is very good, except for the very high concentration clusters. Solid line is our fit, eq. (27), with the last point excluded.

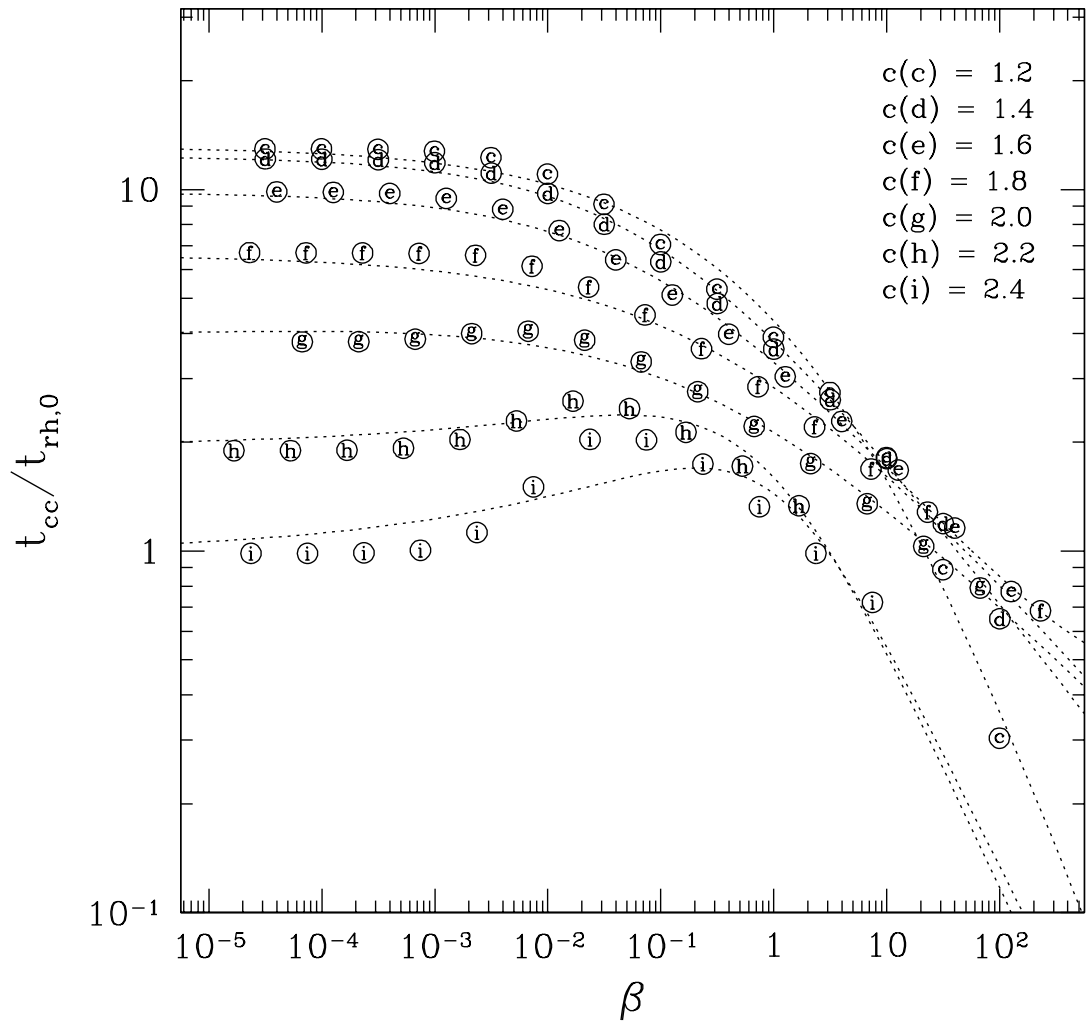


Fig. 18.— The core collapse time as a function of the shock parameter, β . The families of models with the initial concentrations $c = 0.8$ (a) and $c = 1.0$ (b) are excluded for clarity. Dotted lines is our fit, eq. (28).

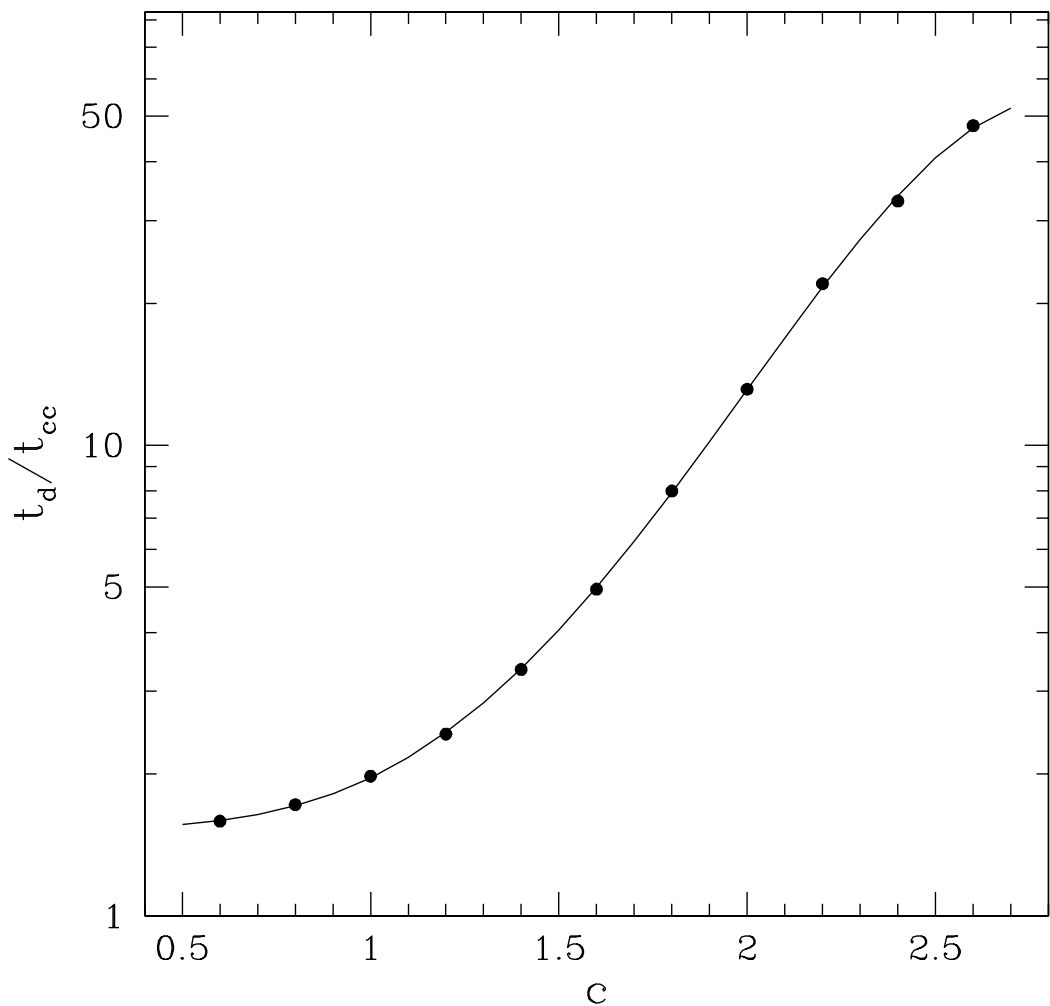


Fig. 19.— Effect of tidal shocks on the cluster total destruction time t_d for several families of the same initial concentrations.

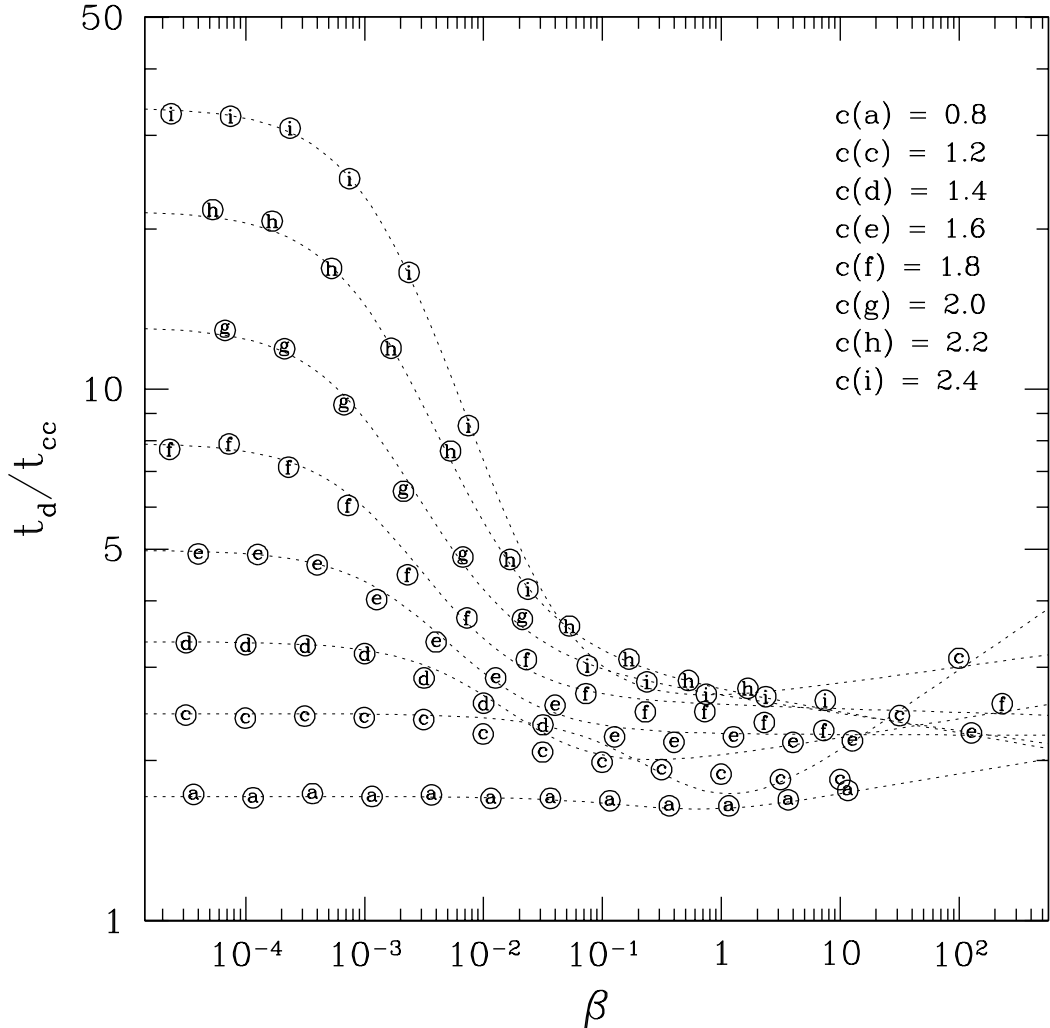


Fig. 20.— The destruction time as a function of the shock parameter, β . For clarity, some of the models are shown only for $\beta \lesssim 0.03$. Dotted lines is our fit, eq. (30).